then suspended in SDS lysis buffer (0.1% SDS, 50 mM Tris–HCl, pH 7.5, 10 mM unbuffered HEPES, 10 mM Na_3VO_4, 4 μg/ml aprotinin, 1.6 μg/ml pepstatin A, 4 μg/ml leupeptin, 1 mM EGTA, and 1 mM PMSF), sonicated, and incubated at 95 °C for 5 min. After Triton X-100 was added to the solution at a final concentration of 0.5%, the resulting lysate was subjected to immunoprecipitation using anti-pTyr antibody-precoated protein-G beads, as described [8,9,38,39,41]. Molecular mass analysis of the trypsinized peptides resulting from tyrosine-phosphorylated proteins was performed by LC/MS/MS.

Results

Formation of nuclear F-actin bundles by nuclear c-Abl

Actin, a major component of the cytoskeleton, is found in the nucleus and its nuclear functions have been reported [18]. To examine the effect of c-Abl on nuclear actin, we overexpressed c-Abl in COS-1 cells and treated the cells with Adriamycin (ADR) and leptomycin B (LMB), which are a DNA-damaging agent and an inhibitor of Crm1-mediated nuclear export, respectively. Consistent with our recent results of endogenous c-Abl [28], nuclear accumulation of overexpressed c-Abl was promoted by treatment with ADR and LMB (Fig. 1A). To co-stain c-Abl and F-actin, cells were briefly extracted with Triton extraction buffer containing 0.4% paraformaldehyde before fixation with 4% paraformaldehyde, because methanol fixation is not suitable for staining of F-actin with phalloidin. The amounts of nuclear F-actin were quantitated using the fluorescence intensity levels of phalloidin staining in the nucleus. Overexpression of c-Abl increased the levels of F-actin not only in the cytoplasm but also in the nucleus, and the levels of nuclear F-actin were further increased by treatment with ADR and LMB (Fig. 1B). Notably, c-Abl was mostly colocalized with nuclear F-actin. These results suggest that nuclear c-Abl is involved in nuclear F-actin formation.

To substantiate the importance of nuclear-localized c-Abl for nuclear F-actin formation, cells were transfected with nuclear-targeted c-Abl (NLS-c-Abl), which is tagged with an additional nuclear localization signal [28]. Even without ADR and LMB treatment, NLS-c-Abl expression was found to increase the levels of nuclear F-actin greater than c-Abl expression (compare Fig. 1C with Fig. 1B). These results suggest that nuclear c-Abl is important for nuclear F-actin formation.

Since c-Abl strongly induces actin polymerization in the cytoplasm [4,5], cytoplasmic F-actin might reflect F-actin staining shown in the nucleus (Fig. 1B and C). Thus, to minimize signal leakage of cytoplasmic F-actin into the nucleus, we reduced the thickness of images from 2.0 μm (Fig. 1B and C) to 0.6 μm (Fig. 1D) and the vertical position of images was set above 4 μm from the bottom of the cells. Despite low intensities due to thin slicing, we confirmed that c-Abl or NLS-c-Abl expression significantly increased the level of nuclear F-actin (Fig. 1D, upper and lower panels). Furthermore, in some (<1%) of the cells transfected with c-Abl, F-actin formation within the nucleus was actually induced by ADR and LMB treatment for 2 h or 12 h, and nuclear F-actin was detected at the middle section (4 μm) but neither at the bottom (0 μm) nor the top section (8 μm) (Fig. 1D, upper panels). In contrast, nuclear intensities of lamin A/C, as an internal control, did not change under these conditions (Fig. 1D, lower panels). These results indicate that thin slicing of images supports the results of Fig. 1B and C in terms of nuclear F-actin formation.

To examine whether inhibition of actin polymerization affected nuclear F-actin formation, cells were treated with latrunculin B (LatB), an inhibitor of actin polymerization [46,47]. NLS-c-Abl-induced nuclear F-actin formation was disrupted by LatB but not by nocodazole (Noc), an inhibitor of microtubule polymerization (Fig. 1E). When cells were cotransfected with GFP-tagged G-actin (GFP-β-actin) and NLS-c-Abl, the bundle formation of GFP-β-actin was also observed by monitoring GFP fluorescence due to the incorporation of GFP-β-actin into nuclear F-actin (Fig. 1F), suggesting that nuclear c-Abl induces nuclear F-actin formation through polymerization of G-actin. Intriguingly, the merged Z-section images revealed that NLS-c-Abl expression induced the formation of long and winding bundles of F-actin within the nucleus (Fig. 1G). Furthermore, NLS-c-Abl was largely colocalized with nuclear F-actin bundles (Fig. 1B and H). The appearance of nuclear F-actin bundles could be seen in control cells despite low levels of nuclear F-actin, and the extent of the formation of nuclear F-actin bundles was positively correlated with the level of nuclear F-actin (Fig. 1H). Although NLS-c-Abl expression increased nuclear F-actin levels in 32.1±4.8% ($n=3$) of the cells (Fig. 1C), nuclear F-actin bundles were all seen in cells exhibiting the increase of nuclear F-actin: cells having faint and thick bundles were 12.0±2.6% ($n=3$) (Fig. 1H, right panels, the first to forth rows) and 20.1±3.6% ($n=3$) (the fifth and sixth rows), respectively. Extraction with 0.1% Triton X-100 and 0.4% HCHO before 4% HCHO fixation was prerequisite for co-staining of nuclear F-actin and nuclear c-Abl [28,this study]. Development of better fixation preserving nuclear F-actin could detect nuclear F-actin bundles more efficiently. Taken together, these results suggest that nuclear c-Abl plays an important role in nuclear F-actin formation.

Inhibition of nuclear F-actin formation by c-Abl knockdown

To examine the role of endogenous c-Abl in nuclear actin dynamics, we generated a stable c-Abl-knockdown cell line (Fig. 2A). c-Abl-knockdown cells transfected with GFP-β-actin were treated with or without ADR and LMB, and F-actin was stained with phalloidin. Expressed GFP-β-actin was colocalized with nuclear F-actin (Fig. 2B). We revealed that the basal levels of nuclear F-actin were slightly but significantly decreased in c-Abl-knockdown cells compared with control cells. Unlike control cells, treatment of c-Abl-knockdown cells with ADR and LMB could barely increase the levels of nuclear F-actin (Fig. 2B). To further ascertain this, we observed thin-slicing sections of images, as shown in Fig. 1D. Upon transfection with mCherry-β-actin, knockdown of endogenous c-Abl significantly decreased the nuclear intensities of F-actin without any change in those of lamin A/C (an internal control) (Fig. 2C). In agreement with the results of Fig. 2B, upon treatment of control cells with ADR and LMB nuclear F-actin was observed at the middle section (4 μm) but neither at the bottom (0 μm) nor the top section (8 μm) (Fig. 2C). Taken together, these results suggest that endogenous c-Abl plays a critical role in nuclear F-actin formation.

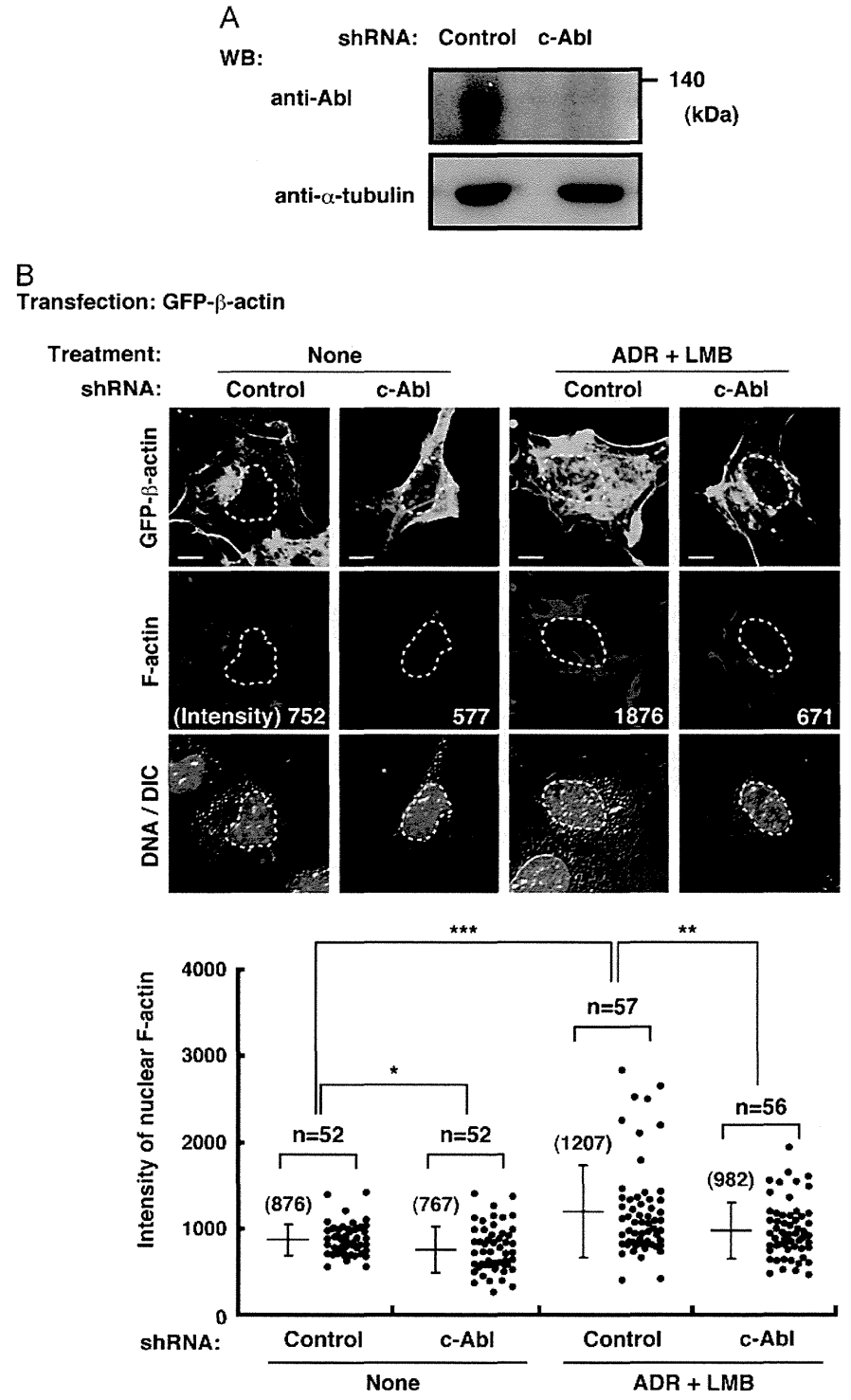


Fig. 2 – Inhibition of nuclear F-actin bundle formation by knockdown of c-Abl. (A) Whole cell lysates prepared from COS-1 and COS-1/shAbl cells were subjected to Western blotting, using anti-Abl and anti-α-tubulin antibodies. (B) COS-1 and COS-1/shAbl cells transfected with GFP-β-actin were cultured for 24 h in the absence or presence of 1 μg/ml ADR and 5 ng/ml LMB during the last 12 h. Cells were extracted and fixed as described in Fig. 1B, and doubly stained with Alexa Fluor 647-phalloidin and PI. The level of nuclear F-actin in each nucleus was plotted as described in Fig. 1B. Asterisks indicate the significant difference ($^{*}p<0.05$; $^{**}p<0.01$; $^{***}p<0.001$) calculated by Student's *t*-test. n, cell number. (C) COS-1 and COS-1/shAbl cells transfected with mCherry-β-actin were cultured for 24 h in the presence or absence of 1 μg/ml ADR and 5 ng/ml LMB during the last 2 h. Cells were extracted and fixed as described in Fig. 1B, and doubly stained with Alexa Fluor 488-phalloidin and anti-lamin A/C. Z-section images (thickness, 0.6 μm) of a representative cell are shown and the levels of nuclear F-actin and lamin A/C in each nucleus were quantitated in the image at 4 μm from the bottom of the cells (0 μm), as described in Fig. 1D. Scale bars, 10 μm. Asterisks indicate the significant difference ($^{*}p<0.05$; $^{**}p<0.01$; $^{***}p<0.001$; NS, not significant) calculated by Student's *t*-test. *n*, cell number.

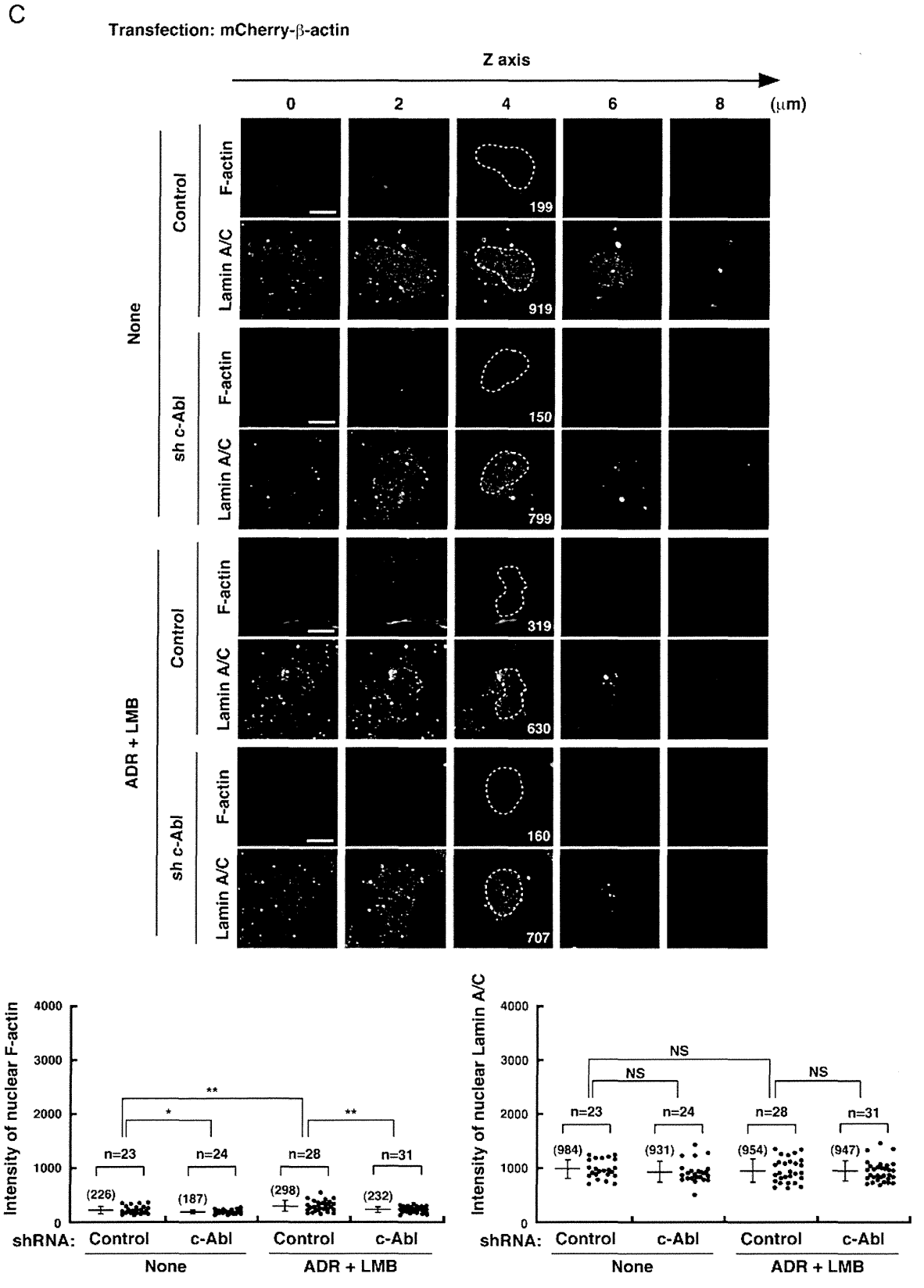


Fig. 2 – (*continued*)

Requirement of c-Abl kinase activity for nuclear F-actin bundle formation

To examine whether the tyrosine kinase activity of nuclear c-Abl was required for nuclear F-actin formation, cells were transfected with NLS-c-Abl and cultured in the presence of various kinase inhibitors. The formation of long and winding nuclear F-actin bundles was specifically inhibited by imatinib (Abl inhibitor) but was not affected by PP2 (Src inhibitor), U0126 (MEK inhibitor), or wortmannin (PI3K inhibitor) (Fig. 3A). Note that imatinib did not affect the increased levels of nuclear F-actin. Furthermore, increased levels of nuclear F-actin were also seen in cells transfected with the kinase-inactive mutant NLS-c-Abl(K290R) (Fig. 3B). Taken together, these results suggest that the levels of nuclear F-actin are increased by the presence of nuclear c-Abl per se but the formation of long and winding nuclear F-actin bundles requires the kinase activity of c-Abl.

To examine the involvement of different tyrosine kinases other than c-Abl in nuclear F-actin bundle formation, cells were transfected with NLS-Lyn and NLS-Syk, which induce nuclear tyrosine phosphorylation [10,28]. We found that NLS-Lyn and NLS-Syk did not increase the levels of nuclear F-actin nor induced the formation of long and winding nuclear F-actin bundles (Fig. 3C). Moreover, we examined whether NLS-c-Abl expression increased the levels of nuclear F-actin in cell types other than monkey kidney fibroblast COS-1 cells. Human epithelial carcinoma HeLa cells and mouse embryonic fibroblast NIH3T3 cells also exhibited the formation of long and winding nuclear F-actin

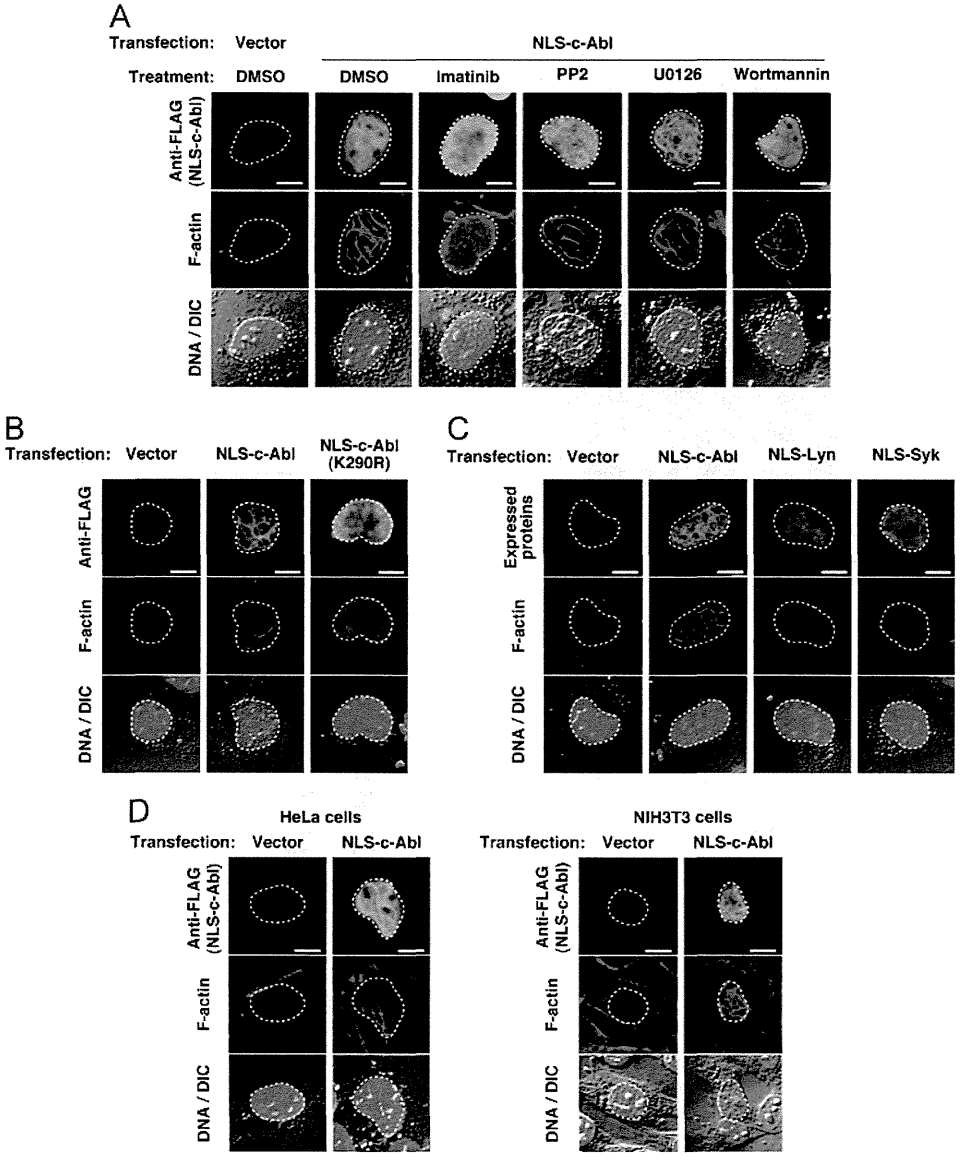


Fig. 3 – Requirement of c-Abl tyrosine kinase activity for nuclear F-actin bundle formation. Cells were transfected as indicated below. Then, cells were extracted, fixed and stained, as described in Fig. 1C. Scale bars, 10 μm. (A) COS-1 cells transfected with vector alone or NLS-c-Abl were cultured for 24 h in the presence of DMSO, 10 μM imatinib, 10 μM PP2, 20 μM U0126, or 100 nM wortmannin during the last 12 h. (B) COS-1 cells transfected with vector alone, NLS-c-Abl, or NLS-c-Abl(K290R) were cultured for 24 h. (C) COS-1 cells transfected with vector alone, NLS-c-Abl, NLS-Lyn, or NLS-Syk were cultured for 24 h. (D) HeLa and NIH3T3 cells transfected with vector alone or NLS-c-Abl were cultured for 24 h.

bundles upon NLS-c-Abl expression (Fig. 3D). These results suggest that unlike Lyn and Syk, the tyrosine kinase activity of c-Abl in the nucleus is required for the formation of long and winding nuclear F-actin bundles in various cell types.

NLS-c-Abl-mediated nuclear tyrosine phosphorylation

Next, to visualize tyrosine phosphorylation in cells exhibiting nuclear F-actin formation, we stained cells with anti-pTyr antibody. While tyrosine-phosphorylated proteins were distributed throughout the nucleus, they were rather abundant at the nuclear periphery in NLS-c-Abl-expressing cells (Fig. 4A). However, nuclear tyrosine-phosphorylated proteins appeared to colocalize with nuclear F-actin bundles only to some extent. In addition, we confirmed that tyrosine phosphorylation was not detected in cells transfected with NLS-c-Abl(K290R) where the levels of nuclear F-actin were increased at the periphery of the nucleus (Fig. 4A). These results suggest that the formation of long and winding nuclear F-actin bundles may involve c-Abl-mediated tyrosine phosphorylation on nuclear F-actin bundles and at the nuclear periphery.

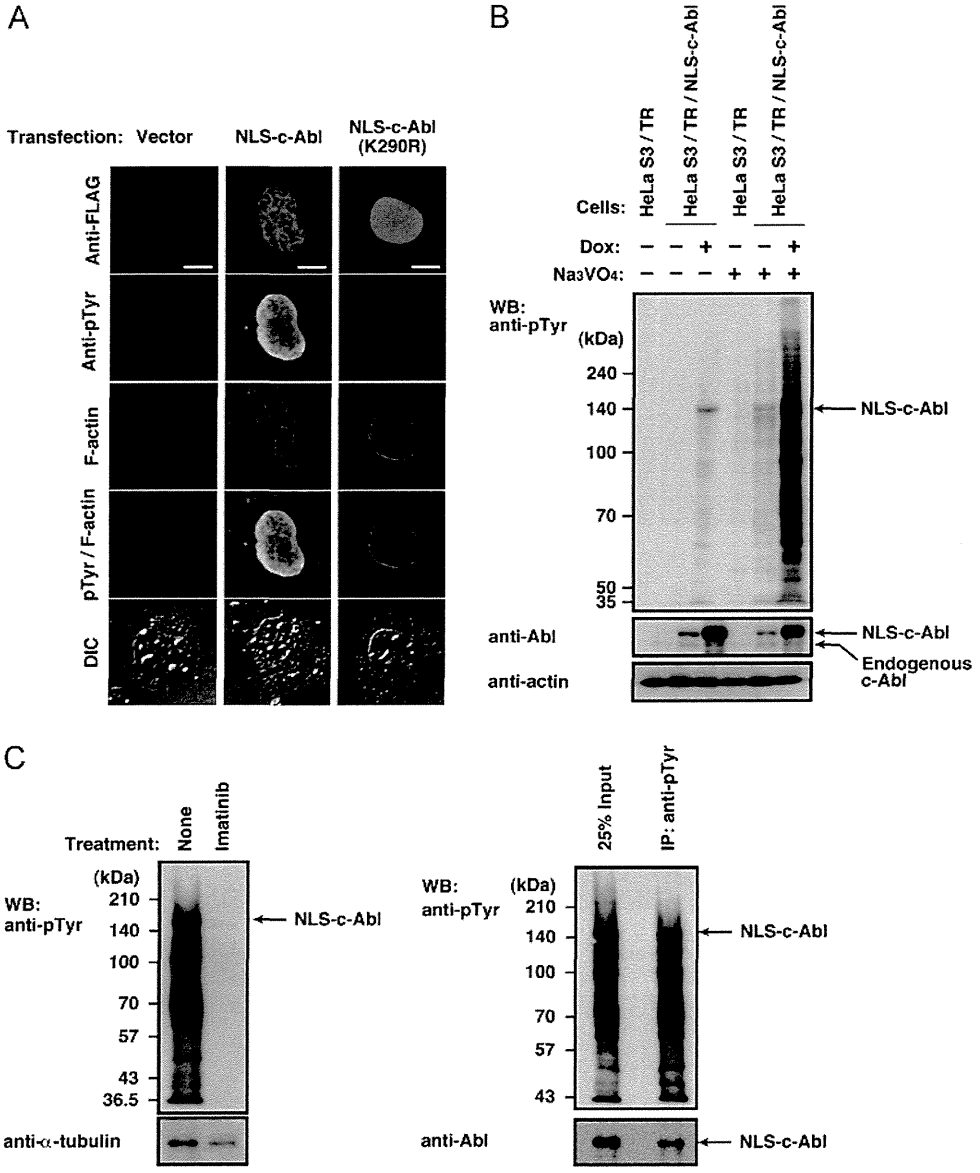


Fig. 4 – Visualization of NLS-c-Abl-mediated tyrosine phosphorylation. (A) COS-1 cells transfected with vector alone, NLS-c-Abl, or NLS-c-Abl(K290R) were cultured for 24 h. Cells were extracted and fixed as described in Fig. 1B, and triply stained with anti-FLAG and anti-pTyr antibodies and Alexa Fluor 647-phalloidin. The resulting red emission of TRITC-stained FLAG is pseudo-colored as blue. Scale bars, 10 μm. (B) Parental HeLa S3/TR cells and HeLa S3/TR/NLS-c-Abl cells treated with or without 1 μg/ml Dox for 24 h were incubated in the presence or absence of 0.5 mM Na_3VO_4 during the last 1 h. Whole cell lysates were subjected to Western blotting, using anti-pTyr, anti-Abl, and anti-actin antibodies. (C) HeLa S3/TR/NLS-c-Abl cells treated with 1 μg/ml Dox plus DMSO or 10 μM imatinib were cultured for 24 h in the presence of 0.5 mM Na_3VO_4 during the last 1 h. Cell lysates prepared as described under 'Materials and Methods' were subjected to Western blotting, using anti-pTyr and anti-α-tubulin antibodies. Tyrosine-phosphorylated proteins were immunoprecipitated with anti-pTyr antibody. Western blotting was performed using anti-pTyr and anti-Abl antibodies.

To analyze NLS-c-Abl-mediated tyrosine-phosphorylated proteins, we incubated cells in medium supplemented with Na_3VO_4, a tyrosine phosphatase inhibitor. Although tyrosine phosphorylation was hardly detected upon induction of NLS-c-Abl, treatment of NLS-c-Abl-induced cells with Na_3VO_4 ensured the detection of tyrosine phosphorylation mediated by NLS-c-Abl (Fig. 4B), suggesting that nuclear tyrosine-phosphorylated proteins are rapidly dephosphorylated. Furthermore, we were able to immunoprecipitate tyrosine-phosphorylated proteins from the cell lysate (Fig. 4C) and then tried to identify the immunoprecipitated proteins by LC/MS/MS analysis. However, we could not find any tyrosine-phosphorylated proteins that are known to regulate actin dynamics. These results suggest that yet unidentified nuclear substrates for c-Abl may be located far upstream of the signal cascade leading to nuclear F-actin bundles formation.

Indispensability of the c-Abl actin-binding domain in nuclear F-actin formation

NLS-c-Abl was largely colocalized to long and winding nuclear F-actin bundles (Figs. 1D, G, 3A–D, 4A, 5C and D). To examine the role of the c-Abl actin-binding domain in nuclear F-actin formation, we constructed the NLS-c-AblΔC mutant, which lacks the C-terminus containing the actin-binding domain (Fig. 5A). Like NLS-c-Abl, NLS-c-AblΔC was found to have the full tyrosine kinase activity (Fig. 5B). Immunostaining showed that tyrosine phosphorylation induced by NLS-c-AblΔC was largely seen at the nuclear periphery, similar to that induced by NLS-c-Abl, although a lack of the C-terminus appeared to change c-Abl's subnuclear localization (Fig. 5C). Despite its full kinase activity, NLS-c-AblΔC was incapable of inducing nuclear F-actin formation, including long and winding nuclear F-actin bundle formation (Fig. 5C, D). The levels of nuclear F-actin in NLS-c-AblΔC-expressing cells were similar to those in control cells. These results suggest that the actin-binding domain of c-Abl plays a critical role in formation of nuclear F-actin.

Next, to examine the effect of c-Abl on nuclear translocation of G-actin and formation of nuclear F-actin, we cotransfected COS-1 cells with GFP-β-actin plus vector, GFP-β-actin plus NLS-c-Abl, GFP-β-actin plus NLS-c-Abl(K290R), or GFP-β-actin plus NLS-c-AblΔC, and monitored the GFP fluorescence of GFP-β-actin in living cells (no extraction) and Triton X-100-extracted cells. NLS-c-Abl, NLS-c-Abl(K290R) and NLS-c-AblΔC were all found to have the ability to translocate GFP-β-actin into the nucleus (Fig. 5E, upper panels, no extraction). Unlike NLS-c-Abl and NLS-c-Abl(K290R), NLS-c-AblΔC was unable to induce nuclear F-actin formation (Fig. 5E, lower panels, Triton X-100 extraction). Consistent with the results of phalloidin staining, only NLS-c-Abl induced the formation of F-actin bundles within the nucleus. These results indicate that c-Abl contributes to nuclear translocation of G-actin and formation of nuclear F-actin.

Furthermore, to examine the positional relationship between nuclear F-actin bundles and chromatin structures, cells were doubly stained for F-actin and DNA upon NLS-c-Abl expression. Serial Z-section images showed that nuclear F-actin bundles appeared to run in the interchromosomal space and stay close to condensed chromatin regions (Fig. 5F). These results suggest that nuclear F-actin bundles may dynamically associate with heterochromatic regions.

Discussion

Non-receptor-type tyrosine kinases largely localize to the cytoplasm but have been shown to exist in the nucleus [6,8,9,48]. Our recent studies showed that nuclear localization of tyrosine kinases, such as c-Src, Lyn, c-Abl, and the intracellular domain of ErbB4, regulate histone modifications and chromatin structural changes, and that heterochromatin protein 1α (HP1α) association with heterochromatin is downregulated by KRAB-associated protein 1 (KAP1) phosphorylation at Tyr-449, Tyr-458, and Tyr-517 [10,28,49,50]. In the present study, we show for the first time that nuclear c-Abl induces nuclear F-actin formation besides histone modifications and chromatin structural changes. In particular, the tyrosine kinase activity of c-Abl in the nucleus is prerequisite for the exhibition of a characteristic structural feature of nuclear F-actin, i.e. formation of long and winding nuclear F-actin bundles.

c-Abl is known to translocate from the cytoplasm into the nucleus in response to ADR-mediated DNA damage. LMB treatment accumulates c-Abl and G-actin in the nucleus by inhibition of Crm1-mediated nuclear export [11,22]. Using GFP-β-actin, we showed that treatment with ADR and LMB promotes the translocation of G-actin into the nucleus and increases the levels of nuclear F-actin, and also showed that knockdown of endogenous c-Abl significantly decreases nuclear F-actin (Fig. 2B). We further showed that compared with intact c-Abl, NLS-c-Abl has a strong impact on nuclear F-actin formation (compare Fig. 1C, E–G with Fig. 1B and D), indicating that nuclear localization of c-Abl plays a critical role in nuclear F-actin formation. Moreover, NLS-c-AblΔC, which lacks the actin-binding domain, is incapable of inducing nuclear F-actin formation despite its high tyrosine kinase activity (Fig. 5).

Monitoring the GFP fluorescence of GFP-β-actin revealed that G-actin is translocated from the cytoplasm into the nucleus by NLS-c-Abl, NLS-c-Abl(K290R), and NLS-c-AblΔC (Fig. 5E). Of these, NLS-c-Abl and NLS-c-Abl(K290R) are capable of inducing nuclear F-actin formation. These results suggest that an unidentified domain of c-Abl is involved in nuclear translocation of G-actin. Considering that the c-Abl actin-binding domain is involved in bundling F-actin in vitro [3], our results suggest that the c-Abl actin-binding domain is essential for F-actin bundle formation in the nucleus. Notably, NLS-c-Abl is unique in having the ability to form long and winding nuclear F-actin bundles. When the GFP fluorescence is carefully examined in the nucleus of a living cell (no extraction), one may find nuclear F-actin bundles (Fig. 5E, upper panel, NLS-c-Abl).

What is the role of c-Abl tyrosine kinase activity in nuclear F-actin formation? Even though c-Abl kinase activity is inactivated by imatinib or the kinase-dead mutation, the levels of nuclear F-actin are increased by the presence of c-Abl in the nucleus (Figs. 3A, B and 4A). However, it is evident that inactivation of c-Abl kinase activity completely blocks the formation of long and winding nuclear F-actin bundles. Visualization with anti-pTyr antibody reveals that nuclear tyrosine phosphorylation by nuclear c-Abl is detected throughout the nucleus and high levels of tyrosine phosphorylation are notably seen at the nuclear periphery (Figs. 4A and 5C). Although tyrosine phosphorylation on nuclear F-actin bundles may play a role in formation of nuclear F-actin bundles, tyrosine phosphorylation at the nuclear

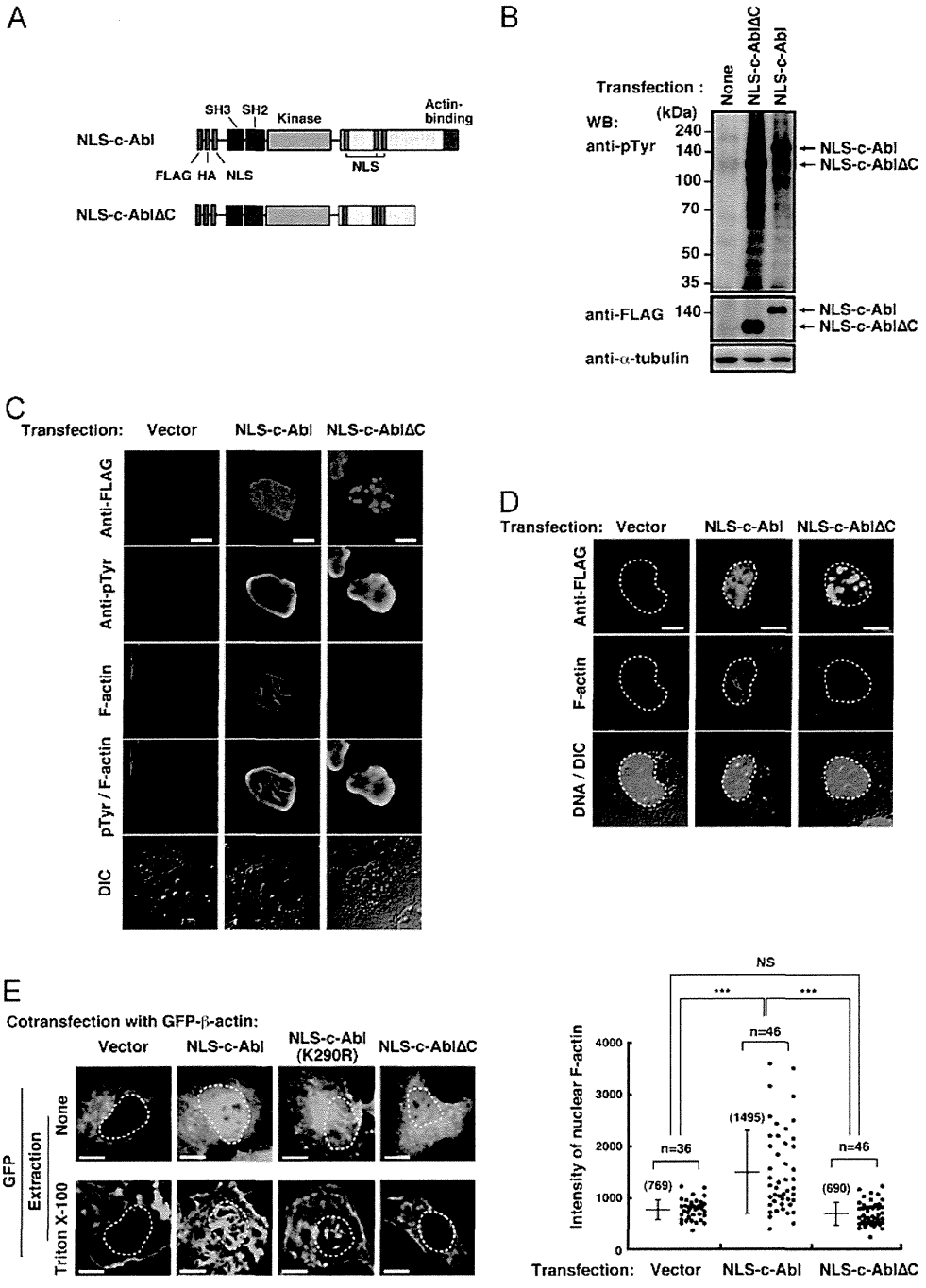


Fig. 5 – Requirement of the actin-binding domain of c-Abl for nuclear F-actin bundle formation. (A) Schematic representations of NLS-c-Abl and NLS-c-AblΔC. FLAG, FLAG-epitope tag; HA, HA-epitope tag; NLS, nuclear localization signal; SH, Src homology domain. (B–D) COS-1 cells transfected with vector alone, NLS-c-Abl, or NLS-c-AblΔC were cultured for 24 h. (B) Whole cell lysates were subjected to Western blotting, using anti-pTyr, anti-FLAG, and anti-α-tubulin antibodies. (C) Cells were extracted, fixed, and stained as described in Fig. 4A. Scale bars, 10 μm. (D) Cells were extracted, fixed and stained, as described in Fig. 1C. Scale bars, 10 μm. The levels of nuclear F-actin were assessed as described in Fig. 1B. Asterisks indicate the significant difference (***$p<0.001$; NS, not significant) calculated by Student's *t*-test. (E) COS-1 cells cotransfected with GFP-β-actin plus vector alone, NLS-c-Abl, NLS-c-Abl(K290R), or NLS-c-AblΔC were cultured for 24 h and extracted with or without 0.1% Triton X-100 in PBS before microscopic observation. Lower panels are displayed with a high sensitivity. Scale bars, 10 μm. (F) COS-1 cells transfected with NLS-c-Abl were cultured for 24 h. Cells were extracted and fixed as described in Fig. 1B, and doubly stained with Alexa Fluor 488-phalloidin and PI. Z-section images of a representative cell at 0.45-μm intervals (*Z* axis) from the lowest (0 μm) to the highest (2.7 μm) position are shown. Scale bar, 10 μm.

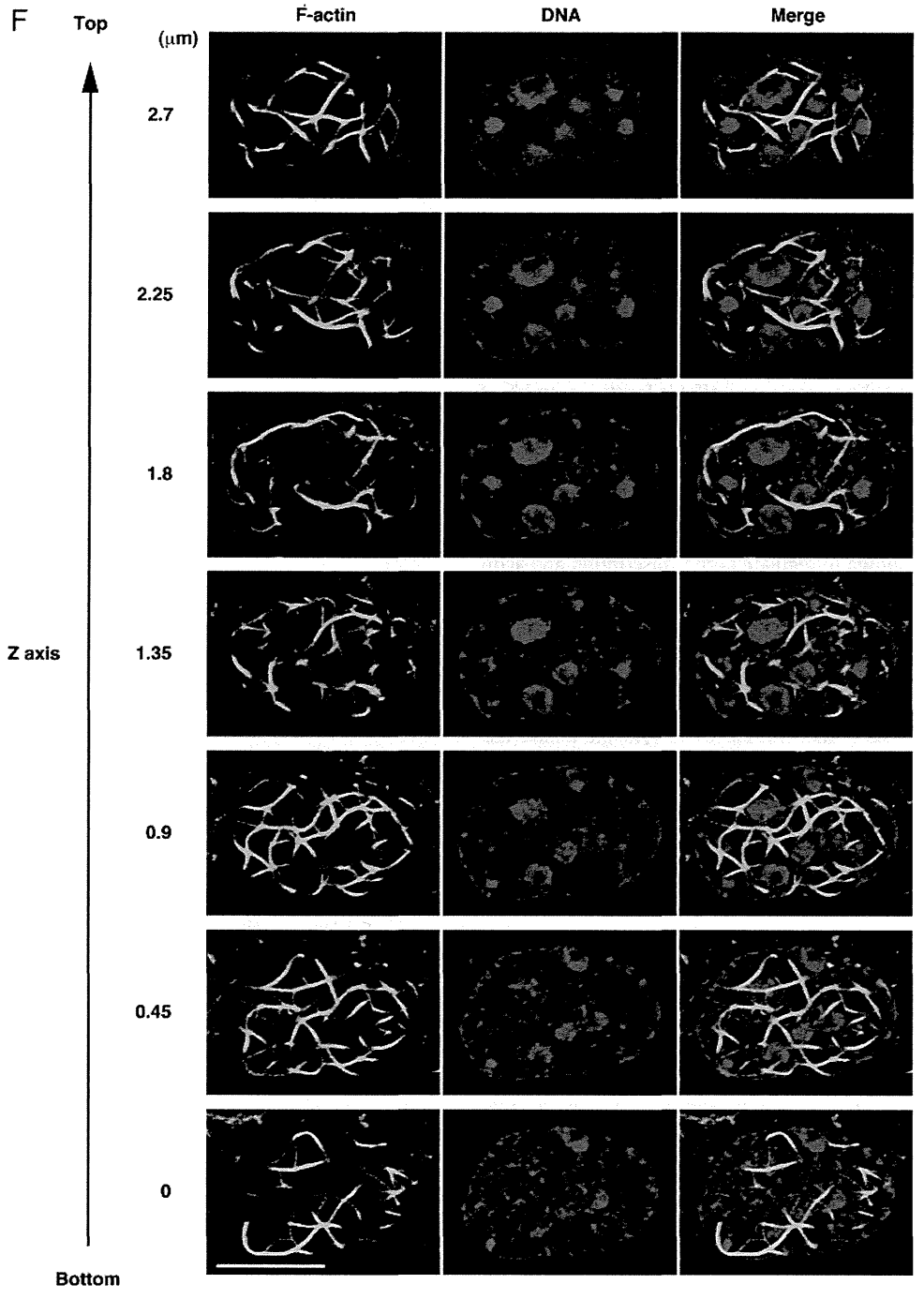


Fig. 5 – (*continued*)

periphery might also have some role in nuclear F-actin bundle formation. Since a large number of proteins are tyrosine-phosphorylated by NLS-c-Abl (Fig. 4B and C), we attempted to identify nuclear substrates for c-Abl by LC/MS/MS analysis. At present, we were unable to find any tyrosine-phosphorylated proteins that are related to actin dynamics. Perhaps c-Abl-mediated tyrosine phosphorylation might occur far upstream of nuclear actin reorganization. We also show that nuclear c-Abl-mediated F-actin formation requires its C-terminal region, which contains the actin-binding domain (Fig. 5A–E). In addition, it is reported that deletion of the Abl C-terminal region reduces c-Abl's sensitivity to imatinib, probably through a change in conformation of its kinase domain [51], leading to the possibility that C-terminal deletion in c-Abl may affect its substrate specificity. Therefore, to compare the difference between substrates for NLS-c-Abl and NLS-c-AblΔC would be helpful in better understanding nuclear actin dynamics.

Posttranslational modifications of histone amino termini by acetylation and methylation regulate chromatin structural changes, such as condensation and decondensation, and gene expression [52–55]. To quantitate the levels of chromatin structural changes, we developed a pixel imaging method utilizing the S.D. value of intensities per pixel upon PI staining for DNA [10]. Using this method, we revealed that nuclear c-Abl induces chromatin

structural changes through heterochromatic histone modifications, including downregulation of histone H4 acetylated on lysine 16 (H4K16Ac) [28]. Importantly, inactivation of NLS-c-Abl tyrosine kinase blocks chromatin structural changes and hypoacetylation of H4K16 [28]. Moreover, nuclear F-actin is reported to associate with chromatin-modifying components, such as histone deacetylases and acetyltransferases, and DNA repair factors, including Ku 70/80 [56,57]. Considering that the formation of long and winding nuclear F-actin bundles is dependent on the tyrosine kinase activity of NLS-c-Abl (Fig. 3A and B) and that the F-actin bundles are located adjacent to chromatin-condensed regions in the interchromosomal space (Fig. 5F), we can imagine that the nuclear F-actin bundles induced by the tyrosine kinase activity of nuclear c-Abl may serve as scaffolds for the assembly of chromatin-remodeling complexes and DNA repair factors through nuclear actin dynamics.

Recent studies have shown that changes in nuclear actin polymerization regulated by cofilin and profilin are important for transcriptional regulation [58–60]. JMY, a transcriptional co-activator of p53, is shown to regulate both transcription and actin filament assembly [61,62]. mDia is also shown to induce nuclear F-actin formation and activates transcription in response to serum stimulation [63]. Taken together, the nuclear F-actin bundle formation mediated by nuclear c-Abl may be deeply involved in transcriptional regulation.

In conclusion, we show that nuclear c-Abl tyrosine kinase has critical roles in nuclear actin dynamics, which depend on the actin-binding domain of c-Abl. In particular, the tyrosine kinase activity of c-Abl is required for the formation of long and winding F-actin bundles within the nucleus. Further studies are required to identify tyrosine-phosphorylated substrates for nuclear c-Abl and understand the roles for c-Abl-induced nuclear F-actin bundle formation in nuclear actin dynamics.

Acknowledgments

We are grateful to Dr. Eli Canaani (Weizmann Institute of Science, Rehovot), Dr. Hiroyuki Miyoshi (RIKEN BRC, Tsukuba), Dr. Toshiki Tamura (National Institute of Infectious Diseases, Tokyo), Dr. Takayuki Yoshimoto (Tokyo Medical University, Tokyo), Dr. Tadashi Yamamoto (The University of Tokyo, Tokyo), Dr. Edward A. Clark (University of Washington, Seattle), Dr. Haruhiko Bito (The University of Tokyo, Tokyo) for their invaluable plasmids and antibodies. We also thank Dr. Naoto Oku (University of Shizuoka, Shizuoka) for helpful suggestions and Yumi Takeda for technical help. This work was supported in part by grants-in-aid for Scientific Research, the Global COE Program (Global Center for Education and Research in Immune Regulation and Treatment) and Special Funds for Education and Research (Development of SPECT probes for Pharmaceutical Innovation) from the Japanese Ministry of Education, Culture, Sports, Science and Technology. K.A., S.K. and K.I. were G-COE Research Assistants, and M.M. is a LGS (Program for Leading Graduate Schools) Research Assistant.

REFERENCES

[1] O. Hantschel, G. Superti-Furga, Regulation of the c-Abl and Bcr-Abl tyrosine kinases, Nat. Rev. Mol. Cell Biol. 5 (2004) 33–44.

[2] A. Sirvent, C. Benistant, S. Roche, Cytoplasmic signalling by the c-Abl tyrosine kinase in normal and cancer cells, Biol. Cell 100 (2008) 617–631.

[3] R.A. Van Etten, P.K. Jackson, D. Baltimore, M.C. Sanders, P.T. Matsudaira, P.A. Janmey, The COOH terminus of the c-Abl tyrosine kinase contains distinct F- and G-actin binding domains with bundling activity, J. Cell Biol. 124 (1994) 325–340.

[4] P.J. Woodring, T. Hunter, J.Y.J. Wang, Regulation of F-actin-dependent processes by the Abl family of tyrosine kinases, J. Cell Sci. 116 (2003) 2613–2626.

[5] Y. Leng, J. Zhang, K. Badour, E. Arpaia, S. Freeman, P. Cheung, M. Siu, K. Siminovitch, Abelson-interactor-1 promotes WAVE2 membrane translocation and Abelson-mediated tyrosine phosphorylation required for WAVE2 activation, Proc. Natl. Acad. Sci. USA 102 (2005) 1098–1103.

[6] C. Cans, R. Mangano, D. Barilá, G. Neubauer, G. Superti-Furga, Nuclear tyrosine phosphorylation: the beginning of a map, Biochem. Pharmacol. 60 (2000) 1203–1215.

[7] G.B.G. Moorhead, L. Trinkle-Mulcahy, A. Ulke-Lemée, Emerging roles of nuclear protein phosphatases, Nat. Rev. Mol. Cell Biol. 8 (2007) 234–244.

[8] N. Yamaguchi, Y. Nakayama, T. Urakami, S. Suzuki, T. Nakamura, T. Suda, N. Oku, Overexpression of the Csk homologous kinase (Chk tyrosine kinase) induces multinucleation: a possible role for chromosome-associated Chk in chromosome dynamics, J. Cell. Sci. 114 (2001) 1631–1641.

[9] K. Ikeda, Y. Nakayama, Y. Togashi, Y. Obata, T. Kuga, K. Kasahara, Y. Fukumoto, N. Yamaguchi, Nuclear localization of Lyn tyrosine kinase mediated by inhibition of its kinase activity, Exp. Cell Res. 314 (2008) 3392–3404.

[10] A. Takahashi, Y. Obata, Y. Fukumoto, Y. Nakayama, K. Kasahara, T. Kuga, Y. Higashiyama, T. Saito, K.K. Yokoyama, N. Yamaguchi, Nuclear localization of Src-family tyrosine kinases is required for growth factor-induced euchromatinization, Exp. Cell Res. 315 (2009) 1117–1141.

[11] S. Taagepera, D. McDonald, J.E. Loeb, L.L. Whitaker, A.K. McElroy, J.Y.J. Wang, T.J. Hope, Nuclear-cytoplasmic shuttling of c-Abl tyrosine kinase, Proc. Natl. Acad. Sci. USA 95 (1998) 7457–7462.

[12] R. Baskaran, L.D. Wood, L.L. Whitaker, C.E. Canman, S.E. Morgan, Y. Xu, C. Barlow, D. Baltimore, A. Wynshaw-Boris, M.B. Kastan, J.Y.J. Wang, Ataxia telangiectasia mutant protein activates c-Abl tyrosine kinase in response to ionizing radiation, Nature 387 (1997) 516–519.

[13] T. Shafman, K.K. Khanna, P. Kedar, K. Spring, S. Kozlov, T. Yen, K. Hobson, M. Gatei, N. Zhang, D. Watters, M. Egerton, Y. Shiloh, S. Kharbanda, D. Kufe, M.F. Lavin, Interaction between ATM protein and c-Abl in response to DNA damage, Nature 387 (1997) 520–523.

[14] Y. Shaul, M. Ben-Yehoyada, Role of c-Abl in the DNA damage stress response, Cell Res. 15 (2005) 33–35.

[15] E. Maiani, M. Diederich, S. Gonfloni, DNA damage response: the emerging role of c-Abl as a regulatory switch?, Biochem. Pharmacol. 82 (2011) 1269–1276.

[16] D. McDonald, G. Carrero, C. Andrin, G. de Vries, M.J. Hendzel, Nucleoplasmic β-actin exists in a dynamic equilibrium between low-mobility polymeric species and rapidly diffusing populations, J. Cell Biol. 172 (2006) 541–552.

[17] N. Visa, P. Percipalle, Nuclear Functions of Actin, Cold Spring Harbor Perspect. Biol. 2 (2010) a000620.

[18] P. de Lanerolle, L. Serebryannyy, Nuclear actin and myosins: life without filaments, Nat. Cell Biol. 13 (2011) 1282–1288.

[19] D.N. Simon, K.L. Wilson, The nucleoskeleton as a genome-associated dynamic 'network of net works', Nat. Rev. Mol. Cell Biol. 12 (2011) 695–708.

[20] P. de Lanerolle, Nuclear actin and myosins at a glance, J. Cell Sci. 125 (2012) 4945–4949.

[21] B.J. Belin, B.A. Cimini, E.H. Blackburn, R.D. Mullins, Visualization of actin filaments and monomers, Mol. Biol. Cell 24 (2013) 982–994.

[22] A. Wada, M. Fukuda, M. Mishima, E. Nishida, Nuclear export of actin: a novel mechanism regulating the subcellular localization of a major cytoskeletal protein, EMBO J. 17 (1998) 1635–1641.
[23] T. Stüven, E. Hartmann, D. Görlich, Exportin 6: a novel nuclear export receptor that is specific for profilin.actin complexes, EMBO J. 22 (2003) 5928–5940.
[24] G. Huet, K.P. Skarp, M.K. Vartiainen, Nuclear actin levels as an important transcriptional switch, Transcription 3 (2012) 1–5.
[25] J. Dopie, K.P. Skarp, E.K. Rajakylä, K. Tanhuanpää, M.K. Vartiainen, Active maintenance of nuclear actin by importin 9 supports transcription, Proc. Natl. Acad. Sci. USA 109 (2012) E544–E552.
[26] E. Shtivelman, B. Lifshitz, R.P. Gale, E. Canaani, Fused transcript of abl and bcr genes in chronic myelogenous leukaemia, Nature 315 (1985) 550–554.
[27] K. Kasahara, Y. Nakayama, Y. Nakazato, K. Ikeda, T. Kuga, N. Yamaguchi, Src signaling regulates completion of abscission in cytokinesis through ERK/MAPK activation at the midbody, J. Biol. Chem. 282 (2007) 5327–5339.
[28] K. Aoyama, Y. Fukumoto, K. Ishibashi, S. Kubota, T. Morinaga, Y. Horiike, R. Yuki, A. Takahashi, Y. Nakayama, N. Yamaguchi, Nuclear c-Abl-mediated tyrosine phosphorylation induces chromatin structural changes through histone modifications that include H4K16 hypoacetylation, Exp. Cell Res. 317 (2011) 2874–2903.
[29] Y. Yamanashi, S. Fukushige, K. Semba, J. Sukegawa, N. Miyajima, K. Matsubara, T. Yamamoto, K. Toyoshima, The yes-related cellular gene lyn encodes a possible tyrosine kinase similar to $p56^{lck}$, Mol. Cell. Biol. 7 (1987) 237–243.
[30] C.L. Law, S.P. Sidorenko, K.A. Chandran, K.E. Draves, A.C. Chan, A. Weiss, S. Edelhoff, C.M. Disteche, E.A. Clark, Molecular cloning of human Syk. A B cell protein-tyrosine kinase associated with the surface immunoglobulin M-B cell receptor complex, J. Biol. Chem. 269 (1994) 12310–12319.
[31] T. Furuyashiki, Y. Arakawa, S. Takemoto-Kimura, H. Bito, S. Narumiya, Multiple spatiotemporal modes of actin reorganization by NMDA receptors and voltage-gated Ca^{2+} channels, Proc. Natl. Acad. Sci. USA 99 (2002) 14458–14463.
[32] T. Kuga, M. Hoshino, Y. Nakayama, K. Kasahara, K. Ikeda, Y. Obata, A. Takahashi, Y. Higashiyama, Y. Fukumoto, N. Yamaguchi, Role of Src-family kinases in formation of the cortical actin cap at the dorsal cell surface, Exp. Cell Res. 314 (2008) 2040–2054.
[33] T. Tamura, T. Kunimatsu, S.T. Yee, O. Igarashi, M. Utsuyama, S. Tanaka, S. Miyazaki, K. Hirokawa, H. Nariuchi, Molecular mechanism of the impairment in activation signal transduction in CD4 T cells from old mice, Int. Immunol. 12 (2000) 1205–1215.
[34] R. Kamath, Z. Jiang, G. Sun, J.C. Yalowich, R. Baskaran, c-Abl kinase regulates curcumin-induced cell death through activation of c-Jun N-terminal kinase, Mol. Pharmacol. 71 (2007) 61–72.
[35] Y. Fukumoto, Y. Obata, K. Ishibashi, N. Tamura, I. Kikuchi, K. Aoyama, Y. Hattori, K. Tsuda, Y. Nakayama, N. Yamaguchi, Cost-effective gene transfection by DNA compaction at pH 4.0 using acidified, long shelf-life polyethylenimine, Cytotechnology 62 (2010) 73–82.
[36] Y. Nakayama, N. Yamaguchi, Multi-lobulation of the nucleus in prolonged S phase by nuclear expression of Chk tyrosine kinase, Exp. Cell Res. 304 (2005) 570–581.
[37] K. Kasahara, Y. Nakayama, A. Kihara, D. Matsuda, K. Ikeda, T. Kuga, Y. Fukumoto, Y. Igarashi, N. Yamaguchi, Rapid trafficking of c-Src, a non-palmitoylated Src-family kinase, between the plasma membrane and late endosomes/lysosomes, Exp. Cell Res. 313 (2007) 2651–2666.
[38] I. Sato, Y. Obata, K. Kasahara, Y. Nakayama, Y. Fukumoto, T. Yamasaki, K.K. Yokoyama, T. Saito, N. Yamaguchi, Differential trafficking of Src, Lyn, Yes and Fyn is specified by the state of palmitoylation in the SH4 domain, J. Cell. Sci. 122 (2009) 965–975.
[39] Y. Obata, Y. Fukumoto, Y. Nakayama, T. Kuga, N. Dohmae, N. Yamaguchi, The Lyn kinase C-lobe mediates Golgi export of Lyn through conformation-dependent ACSL3 association, J. Cell Sci. 123 (2010) 2649–2662.
[40] N. Yamaguchi, M.N. Fukuda, Golgi retention mechanism of ß-1, 4-galactosyltransferase: membrane-spanning domain-dependent homodimerization and association with α- and β-tubulins, J. Biol. Chem. 270 (1995) 12170–12176.
[41] J. Tada, M. Omine, T. Suda, N. Yamaguchi, A common signaling pathway via Syk and Lyn tyrosine kinases generated from capping of the sialomucins CD34 and CD43 in immature hematopoietic cells, Blood 93 (1999) 3723–3735.
[42] K. Kasahara, Y. Nakayama, K. Ikeda, Y. Fukushima, D. Matsuda, S. Horimoto, N. Yamaguchi, Trafficking of Lyn through the Golgi caveolin involves the charged residues on αE and αI helices in the kinase domain, J. Cell Biol. 165 (2004) 641–652.
[43] D. Matsuda, Y. Nakayama, S. Horimoto, T. Kuga, K. Ikeda, K. Kasahara, N. Yamaguchi, Involvement of Golgi-associated Lyn tyrosine kinase in the translocation of annexin II to the endoplasmic reticulum under oxidative stress, Exp. Cell Res. 312 (2006) 1205–1217.
[44] K. Kasahara, Y. Nakayama, I. Sato, K. Ikeda, M. Hoshino, T. Endo, N. Yamaguchi, Role of Src-family kinases in formation and trafficking of macropinosomes, J. Cell. Physiol. 211 (2007) 220–232.
[45] G. Huyer, S. Liu, J. Kelly, J. Moffat, P. Payette, B. Kennedy, G. Tsaprailis, M.J. Gresser, C. Ramachandran, Mechanism of inhibition of protein-tyrosine phosphatases by vanadate and pervanadate, J. Biol. Chem. 272 (1997) 843–851.
[46] I. Spector, N.R. Shochet, Y. Kashman, A. Groweiss, Latrunculins: novel marine toxins that disrupt microfilament organization in cultured cells, Science 219 (1983) 493–495.
[47] T. Wakatsuki, B. Schwab, N.C. Thompson, E.L. Elson, Effects of cytochalasin D and latrunculin B on mechanical properties of cells, J. Cell Sci. 114 (2001) 1025–1036.
[48] F. Zhou, J. Hu, H. Ma, M.L. Harrison, R.L. Geahlen, Nucleocytoplasmic trafficking of the syk protein tyrosine kinase, Mol. Cell. Biol. 26 (2006) 3478–3491.
[49] K. Ishibashi, Y. Fukumoto, H. Hasegawa, S. Kubota, K. Aoyama, S. Kubota, Y. Nakayama, N. Yamaguchi, Nuclear ErbB4 signaling through H3K9me3 is antagonized by EGFR-activated c-Src, J. Cell Sci. 126 (2013) 625–637.
[50] S. Kubota, Y. Fukumoto, K. Aoyama, K. Ishibashi, R. Yuki, T. Morinaga, T. Honda, N.-t. Yamaguchi, T. Kuga, T. Tomonaga, N. Yamaguchi, Phosphorylation of KRAB-associated protein 1 (KAP1) at Tyr-449, Tyr-458, and Tyr-517 by nuclear tyrosine kinases inhibits the association of KAP1 and heterochromatin protein 1α (HP1α) with heterochromatin, J. Biol. Chem. 288 (2013) 17871–17883.
[51] M. Preyer, P. Vigneri, J.Y.J. Wang, Interplay between kinase domain autophosphorylation and F-actin binding domain in regulating imatinib sensitivity and nuclear import of BCR-ABL, PLoS One 6 (2011) e17020.
[52] M. Grunstein, Histone acetylation in chromatin structure and transcription, Nature 389 (1997) 349–352.
[53] A.I. Lamond, W.C. Earnshaw, Structure and function in the nucleus, Science 280 (1998) 547–553.
[54] B.D. Strahl, C.D. Allis, The language of covalent histone modifications, Nature 403 (2000) 41–45.
[55] T. Jenuwein, C.D. Allis, Translating the histone code, Science 293 (2001) 1074–1080.
[56] C. Andrin, M.J. Hendzel, F-actin-dependent insolubility of chromatin-modifying components, J. Biol. Chem. 279 (2004) 25017–25023.
[57] C. Andrin, D. McDonald, K.M. Attwood, A. Rodrigue, S. Ghosh, R. Mirzayans, J.Y. Masson, G. Dellaire, M.J. Hendzel, A requirement for polymerized actin in DNA double-strand break repair, Nucleus 3 (2012) 384–395.

[58] A. Obrdlik, P. Percipalle, The F-actin severing protein cofilin-1 is required for RNA polymerase II transcription elongation, Nucleus 2 (2011) 72–79.
[59] E. Söderberg, V. Hessle, A. von Euler, N. Visa, Profilin is associated with transcriptionally active genes, Nucleus 3 (2012) 290–299.
[60] P. Percipalle, Co-transcriptional nuclear actin dynamics, Nucleus 4 (2013) 43–52.
[61] J.B. Zuchero, A.S. Coutts, M.E. Quinlan, N.B. La Thangue, R.D. Mullins, p53-cofactor JMY is a multifunctional actin nucleation factor, Nat. Cell Biol. 11 (2009) 451–459.
[62] J.B. Zuchero, B. Belin, R.D. Mullins, Actin binding to WH2 domains regulates nuclear import of the multifunctional actin regulator JMY, Mol. Biol. Cell 23 (2012) 853–863.
[63] C. Baarlink, H. Wang, R. Grosse, Nuclear actin network assembly by formins regulates the SRF coactivator MAL, Science 340 (2013) 864–867.

THE JOURNAL OF BIOLOGICAL CHEMISTRY VOL. 288, NO. 24, pp. 17871–17883, June 14, 2013
© 2013 by The American Society for Biochemistry and Molecular Biology, Inc. Published in the U.S.A.

Phosphorylation of KRAB-associated Protein 1 (KAP1) at Tyr-449, Tyr-458, and Tyr-517 by Nuclear Tyrosine Kinases Inhibits the Association of KAP1 and Heterochromatin Protein 1α (HP1α) with Heterochromatin*[S]

Received for publication, November 19, 2012, and in revised form, May 2, 2013 Published, JBC Papers in Press, May 4, 2013, DOI 10.1074/jbc.M112.437756

Sho Kubota[‡1], **Yasunori Fukumoto**[‡], **Kazumasa Aoyama**[‡1], **Kenichi Ishibashi**[‡1], **Ryuzaburo Yuki**[‡], **Takao Morinaga**[‡1], **Takuya Honda**[‡], **Noritaka Yamaguchi**[‡], **Takahisa Kuga**[§], **Takeshi Tomonaga**[§], **and Naoto Yamaguchi**[‡2]

From the [‡]*Department of Molecular Cell Biology, Graduate School of Pharmaceutical Sciences, Chiba University, Inohana 1-8-1, Chuo-ku, Chiba 260-8675, Japan and the* [§]*Laboratory of Proteome Research, National Institute of Biomedical Innovation, Ibaraki, Osaka 567-0085, Japan*

Background: We showed that nuclear tyrosine phosphorylation is involved in chromatin structural changes.
Results: Several tyrosine kinases phosphorylate KAP1 at Tyr-449, Tyr-458, and Tyr-517 in the nucleus, resulting in a decrease of KAP1 association with heterochromatin.
Conclusion: Tyrosine phosphorylation of KAP1 by nucleus-localized tyrosine kinases, including Src, involves heterochromatin structural changes.
Significance: These findings provide a new insight into nuclear tyrosine phosphorylation signals.

Protein tyrosine phosphorylation regulates a wide range of cellular processes at the plasma membrane. Recently, we showed that nuclear tyrosine phosphorylation by Src family kinases (SFKs) induces chromatin structural changes. In this study, we identify KRAB-associated protein 1 (KAP1/TIF1β/TRIM28), a component of heterochromatin, as a nuclear tyrosine-phosphorylated protein. Tyrosine phosphorylation of KAP1 is induced by several tyrosine kinases, such as Src, Lyn, Abl, and Brk. Among SFKs, Src strongly induces tyrosine phosphorylation of KAP1. Nucleus-targeted Lyn potentiates tyrosine phosphorylation of KAP1 compared with intact Lyn, but neither intact Fyn nor nucleus-targeted Fyn phosphorylates KAP1. Substitution of the three tyrosine residues Tyr-449/Tyr-458/Tyr-517, located close to the HP1 binding-motif, into phenylalanine ablates tyrosine phosphorylation of KAP1. Immunostaining and chromatin fractionation show that Src and Lyn decrease the association of KAP1 with heterochromatin in a kinase activity-dependent manner. KAP1 knockdown impairs the association of HP1α with heterochromatin, because HP1α associates with KAP1 in heterochromatin. Intriguingly, tyrosine phosphorylation of KAP1 decreases the association of HP1α with heterochromatin, which is inhibited by replacement of endogenous KAP1 with its phenylalanine mutant (KAP1-Y449F/Y458F/Y517F, KAP1–3YF). In DNA damage, KAP1–3YF repressed transcription of p21. These results suggest that nucleus-localized tyrosine kinases, including SFKs, phosphorylate KAP1 at Tyr-449/Tyr-458/Tyr-517 and inhibit the association of KAP1 and HP1α with heterochromatin.

Protein tyrosine phosphorylation is one of the key post-translational modifications that controls a wide variety of cellular events, such as cell proliferation, differentiation, gene transcription, and cell adhesion (1, 2). Although it is well known that tyrosine phosphorylation is important for signal transduction at the plasma membrane, the role of nuclear tyrosine phosphorylation in nuclear events is poorly understood (3, 4).

Human genome encodes 518 protein kinases, which consist of 428 serine and threonine kinases and 90 tyrosine kinases (5). Receptor-type tyrosine kinases transmit signals from the extracellular milieu to the inside of the cell. On the other hand, the function of non-receptor-type tyrosine kinases is influenced by their intracellular localization (6). Src family kinases (SFKs),[3] which belong to a family of non-receptor-type tyrosine kinases, consist of proto-oncogene products and structurally related proteins, such as c-Src, Lyn, and Fyn (7, 8). Recently, we showed that SFKs are imported into and rapidly exported from the nucleus (9, 10). Brk (breast tumor kinase), an Src-related kinase, is localized to the cytoplasm and the nucleus (11). The proto-oncogene product c-Abl, a non-receptor-type tyrosine kinase, can shuttle between the cytoplasm and the nucleus (12). ErbB4, a member of ErbB receptor tyrosine kinases, is cleaved upon ligand stimulation, and the intracellular domain is released into the cytoplasm and the nucleus (13).

Recently, we reported that nucleus-localized tyrosine kinases, such as SFK, Abl, Chk, and ErbB4, play roles in the

* This work was supported in part by grants-in-aid for scientific research, the Global Center for Education and Research in Immune Regulation and Treatment (G-COE) Program, and Special Funds for Education and Research (Development of SPECT Probes for Pharmaceutical Innovation) from the Japanese Ministry of Education, Culture, Sports, Science, and Technology.
[S] This article contains supplemental Tables S1 and S2.
[1] A G-COE Research Assistant.
[2] To whom correspondence should be addressed. Tel./Fax: 81-43-226-2868; E-mail: nyama@faculty.chiba-u.jp.

[3] The abbreviations used are: SFK, Src family kinase; NLS, nuclear localization signal; KD, kinase-dead; H3K9me3, histone H3 trimethylated on lysine 9; TRITC, tetramethylrhodamine isothiocyanate; ADR, Adriamycin; PI, propidium iodide; KAP1-wt, wild-type KAP1; KAP1–3YF, KAP1-Y449F/Y458F/Y517F mutant.

Downloaded from http://www.jbc.org/ at IYAKU KIBAN KENKYUJO on April 24, 2014

regulation of chromatin structure and histone modifications through tyrosine phosphorylation (10, 14–17). To substantiate the involvement of nuclear tyrosine kinases in chromatin structural changes, we constructed mutants with a nuclear localization signal (NLS). Compared with the intact form of tyrosine kinases, NLS-SFK, NLS-c-Abl, and NLS-4ICD (NLS-tagged ErbB4 intracellular domain) have strong effects on chromatin structural changes (10, 16, 17). NLS-tagged tyrosine kinases help us to understand the relationships between tyrosine kinases and chromatin structural changes. However, it is still unclear how chromatin structure is regulated through tyrosine phosphorylation.

In this study, we sought to identify nuclear tyrosine-phosphorylated proteins that are related to chromatin structural changes and found a candidate protein called KRAB-associated protein 1 (KAP1/TIF1β/Trim28). We revealed that three tyrosine residues of KAP1 are the common tyrosine phosphorylation sites for various tyrosine kinases localizing in the nucleus. We further showed that tyrosine phosphorylation of KAP1 decreases the amounts of chromatin-bound KAP1 and HP1α. In addition, tyrosine phosphorylation of KAP1 is involved in transcription of p21 upon DNA damage.

EXPERIMENTAL PROCEDURES

Plasmids—Intact c-Src, c-Src (c-Src-HA), and NLS-Src were constructed from cDNA encoding human wild-type Src (18) (provided by D. J. Fujita) as described (10, 19). Intact Lyn, Lyn (Lyn-HA), Lyn-K275A (Lyn(KD)-HA, KD indicating kinase-dead), NLS-Lyn, and NLS-Lyn-K275A (NLS-Lyn(KD)) were constructed from cDNA encoding human wild-type Lyn (20) (provided by T. Yamamoto) as described (10, 19). To construct pOZ-NLS-Lyn, cDNA encoding human wild-type Lyn was subcloned into the XhoI-NotI site of the pOZ-FLAG-HA-N vector (21) (provided by A. Iwama). NLS was inserted between the HA epitope and Lyn. The sequence GGL was inserted between the HA epitope and the NLS. The sequence LDPAQWRPRDPLC-WTRPAAPKLSPRAGN was inserted between the NLS and Lyn. pOZ-NLS-Lyn-K275R/Y508F(KD), in which the ATP binding site and the negative regulatory site were mutated, was created by PCR using pOZ-NLS-Lyn as a template. Intact Fyn and NLS-Fyn were constructed from cDNA encoding human wild-type Fyn (22) (provided by T. Yamamoto) as described (10, 19). NLS-4ICD was constructed from cDNA encoding human ErbB4 CYT-1 (23) (provided by S. Yokoyama) as described (17). NLS-c-Abl was constructed from cDNA encoding human wild-type c-Abl-1b (24) (provided by E. Canaani) as described (16). NLS-Syk was constructed from cDNA encoding human wild-type Syk (25) (provided by E. A. Clark) as described (10). cDNA encoding human Brk (Open Biosystems) was subcloned into the pcDNA4/TO-FH vector (16). Myc-JMJD2a was constructed from cDNA containing human wild-type JMJD2a and subcloned into the Myc-pcDNA3 vector. Wild-type KAP1 (FLAG-KAP1-wt), FLAG-KAP1(N1)(1–469), and FLAG-KAP1(C)(469–835) were gifts from H. Ariga (26). FLAG-KAP1(N2)(1–380) was constructed from FLAG-KAP1(N1)(1–469) by digesting with BamHI, blunting, and ligation. The Tyr → Phe mutants of KAP1 were created by PCR using KAP1-wt as a template with the primers (supplemental Table S1).

RNA Interference—Knockdown of KAP1 was performed with short hairpin RNA (shRNA) for silencing KAP1 (5′- gcatgaaccccttgtgctg-3′) (27). The nucleotides for shRNA were annealed and subcloned into the BglII-XbaI site of the pENTR4/H1 vector (provided by H. Miyoshi) (28, 29). To establish a KAP1-stable knockdown cell line, HeLa S3 cells were co-transfected with pENTR4/H1/shKAP1 and a plasmid containing the hygromycin-resistant gene and selected in 250 μg/ml hygromycin. To replace endogenous KAP1 with KAP1-wt or KAP1–3YF mutant, KAP1 knockdown cells were transfected with knockdown-resistant KAP1-wt or KAP1–3YF, and cell clones expressing KAP1-wt or KAP1–3YF were selected in 300 μg/ml G418. shRNA-resistant KAP1 constructs were made by mutation of the shRNA target site by PCR using KAP1 as a template with the sense primer 5′- acacaagcatgaaccactagtactgttttgtgagagctgtgatactc-3′ and the antisense primer 5′-ctctcacaaaacagtactagtggttcatgcttgtgtacgttgcaata-3′.

Antibodies—The following antibodies were used: Tyr(P) (4G10 and polyclonal antibody; Upstate Biotechnology, Inc.; provided by T. Tamura and T. Yoshimoto (30)), Lyn (Lyn9; Wako Pure Chemical Industries (Osaka, Japan) and Lyn44 (Santa Cruz Biotechnology, Inc., Santa Cruz, CA)), FLAG (M2 and polyclonal antibody; Sigma), HA (Y11; Santa Cruz Biotechnology, Inc.), actin (clone C4; CHEMICON International), α-tubulin (MCA78G; Serotec), Src phosphorylated on Tyr-416 (Cell Signaling Technology), KAP1 (ab10484; Abcam and Bethyl Laboratories), HP1α (05-689; Millipore), histone H3 trimethylated on lysine 9 (H3K9me3) (ab8898; Abcam), Syk (4D10; Santa Cruz Biotechnology, Inc.), Brk (C-18; Santa Cruz Biotechnology, Inc.), Abl (8E9; BD Pharmingen), Fyn (Fyn3; Santa Cruz Biotechnology, Inc.), Src (GD11; Upstate Biotechnology, Inc.), Ku70 (C-19; Santa Cruz Biotechnology, Inc.), ErbB4 (C-18; Santa Cruz Biotechnology, Inc.), Chk2 (DCS-273; Medical and Biological Laboratories), Chk2-pT68 (Cell Signaling Technology), KAP1-Ser(P)-473 (BioLegend), KAP1-Ser(P)-824 (Bethyl Laboratories), and lamin A/C (N-18; Santa Cruz Biotechnology, Inc.). Horseradish peroxidase (HRP)-F(ab′)$_2$ secondary antibodies were purchased from Amersham Biosciences. FITC-IgG, TRITC-IgG, and Alexa Fluor 488-, Alexa Fluor 546-, and Alexa Fluor 647-labeled IgG secondary antibodies were purchased from BioSource International, Sigma-Aldrich, and Invitrogen.

Cells and Transfection—Cells were cultured in Iscove's modified DME medium containing 5% bovine serum (COS-1 and HeLa S3 cells; Japanese Collection of Research Bioresources, Osaka). Cells seeded in a 35-mm (60-mm) culture dish were transiently transfected with 1 μg (3 μg) of plasmid DNA using 5 μg (15 μg) of linear polyethyleneimine (25 kDa) (Polyscience, Inc.) (31) or Lipofectamine 2000 (Invitrogen). To generate HeLa S3 cells stably expressing NLS-Lyn or NLS-Lyn(KD), standard transfection and retroviral production procedures were used (21). The infected cells expressing CD25 were enriched by cell sorting. To stimulate tyrosine phosphorylation in HeLa S3/NLS-Lyn, cells were treated with 0.5 mM sodium orthovanadate (Na_3VO_4) for 1.5 h. A HeLa S3 cell clone expressing v-Src was generated in an inducible manner (HeLa S3/TR/v-Src). To induce DNA damage responses, cells were treated with 100 ng/ml Adriamycin (ADR) for 1 h. To inhibit

NLS-Lyn-mediated tyrosine phosphorylation, cells were treated with 10 μM PP2 (Sigma) or 5–10 μM SU6656 (Sigma).

Western Blotting and Immunoprecipitation—Cell lysates were prepared in SDS-PAGE sample buffer or Triton X-100 lysis buffer (30 mM HEPES, pH 7.4, 100 mM NaCl, 0.5% Triton X-100, 4 mM EDTA, 10 mM NaF, 50 μg/ml aprotinin, 100 μM leupeptin, 25 μM pepstatin A, and 2 mM PMSF) and subjected to SDS-PAGE and electrotransferred onto polyvinylidene difluoride membranes (Millipore). Immunodetection was performed by enhanced chemiluminescence (Millipore), as described (32–34). Results were analyzed using a ChemiDoc XRS-Plus image analyzer (Bio-Rad). Immunoprecipitation was performed using antibody-precoated protein G beads, as described (9, 29, 33, 35). The intensity of chemiluminescence was measured using Quantity One software (Bio-Rad). Relative amounts of KAP1, HP1α, and histone H3K9me3 represent means ± S.D. from three independent experiments. *Asterisks* indicate the significant differences (*, $p < 0.05$; **, $p < 0.01$) calculated by Student's *t* test (Fig. 3, *E* and *L*). Composite figures were prepared using the GNU Image Manipulation Program version 2.6.2 software (GIMP) and Illustrator version 14.0 software (Adobe).

Subcellular Fractionation—Cell pellets were washed with phosphate-buffered saline (PBS) and resuspended in low salt buffer (10 mM HEPES, pH 7.4, 10 mM KCl, 0.1% Triton X-100, 0.34 M sucrose, 10% glycerol, 1.7 mM $MgCl_2$, 10 mM NaF, 4 mM β-glycerophosphate, 2 mM Na_3VO_4, 50 μg/ml aprotinin, 100 μM leupeptin, 25 μM pepstatin A, and 2 mM PMSF), and the cells were kept on ice for 10 min. Cytosolic proteins were separated from nuclei by centrifugation at 2,000 × *g* for 5 min. Isolated nuclei were lysed in high salt buffer (50 mM HEPES, pH 7.4, 300 mM KCl, 1.0% Triton X-100, 20% glycerol, 50 mM NaF, 10 mM β-glycerophosphate, 10 mM Na_3VO_4, 1 mM EDTA, 50 μg/ml aprotinin, 100 μM leupeptin, 25 μM pepstatin A, and 2 mM PMSF). After a 20-min incubation on ice, soluble nuclear proteins were separated from chromatin by centrifugation at 17,900 × *g* for 10 min. The resulting chromatin fraction was once washed with high salt buffer, solubilized in SDS sample buffer, and sheared by sonication (36–38).

Immunofluorescence—Confocal and differential interference-contrast images were obtained using a Fluoview Fv500 confocal laser-scanning microscope with a 40 × 1.00 or a 60 × 1.00 numerical aperture water immersion objective (Olympus, Tokyo), as described (15, 16, 39). One planar (*xy*) section slice (0.6- or 2.0-μm thickness) was shown in all experiments. For HP1α and KAP1 staining, cells were extracted with high salt buffer for 3 min on ice and fixed in 100% methanol for 5 min at −20 °C. Cells were permeabilized in PBS containing 0.2% Triton X-100 and 3% bovine serum albumin at room temperature (40). Cells were subsequently reacted with appropriate primary antibodies for 1 h, washed with PBS containing 0.1% saponin, and stained with FITC-, TRITC-, Alexa Fluor 488-, Alexa Fluor 546-, or Alexa Fluor 647-conjugated secondary antibodies for 1 h. For DNA staining, cells were treated with 200 μg/ml RNase A for 1 h and with 20 μg/ml propidium iodide (PI) or 200 nM TOPRO-3 for 30 min and mounted with Prolong Antifade™ reagent (Molecular Probes, Inc.). The resulting red emission of TOPRO-3 and Alexa Fluor 647 are *pseudocolored blue*. Composite figures were prepared using GIMP version 2.6.2 and Illustrator version 14.0. For quantitation of amounts of KAP1 and HP1α, confocal images were obtained using a Fluoview Fv500 confocal laser-scanning microscope, and then fluorescence intensities of immunostaining were measured using ImageJ software (National Institutes of Health). *Bars* represent means ± S.D. from a representative experiment. *Numbers* in *parentheses* indicate mean values, and *asterisks* indicate significant differences (**, $p < 0.01$; ***, $p < 0.001$) calculated by Student's *t* test. *Scale bars* are 10 μm (Figs. 3 (*A–C*), 4 (*B–E*), and 5 (*B–D*)) and 20 μm (Figs. 1*A*, 4*A*, and 5*A*). Because two or three independent experiments gave similar results, a representative experiment is shown.

In Vitro Kinase Assay—Lysates were prepared in Triton X-100 lysis buffer. Immunoprecipitation was performed using anti-FLAG or anti-HA antibody-precoated protein G beads. Immunodetection was performed as reported (41). *In vitro* kinase assays were performed as described (14, 32, 35, 42). In brief, Lyn was immunoprecipitated with anti-HA antibody from Triton X-100 lysates of COS-1 cells transfected with Lyn (Lyn-HA) or Lyn(KD) (Lyn(KD)-HA). After washing, equal amounts of each immunoprecipitate were reacted with FLAG peptide-eluted FLAG-KAP1 in kinase buffer (40 mM HEPES, pH 7.4, 0.1% Triton X-100, 5 mM $MnCl_2$, 5 mM $MgCl_2$, 1 mM Na_3VO_4) containing 100 μM unlabeled ATP at 30 °C for the indicated periods. Phosphorylated bands were immunodetected with anti-Tyr(P) antibody, and the intensity of chemiluminescence was measured using Quantity One software (Bio-Rad). Composite figures were prepared using GIMP version 2.6.2 and Illustrator version 14.0.

Identification of p110 by Peptide Mapping—Parental HeLa S3 or HeLa S3/NLS-Lyn cells were treated with 0.5 mM Na_3VO_4 for 1.5 h and lysed with SDS-lysis buffer (100 mM Tris, pH 6.8, 3% SDS, 20% glycerol, 10 mM Na_3VO_4). Cell lysates were boiled at 95 °C for 5 min and sonicated. To dilute SDS to a concentration of 0.1%, wash buffer (30 mM HEPES, pH 7.4, 300 mM NaCl, 1.0% Triton X-100) was added before immunoprecipitation. Tyrosine-phosphorylated proteins were collected on anti-Tyr(P) antibody-precoated protein G beads from cell lysates. After extensively washing the beads with wash buffer, the immune pellets were analyzed by SDS-PAGE and Coomassie Brilliant Blue staining. The protein band corresponding to p110 was cut out and digested with trypsin (Trypsin Gold; Promega). After the digestion, molecular mass analysis of trypsin fragments was performed by LC/MS/MS. Identification of the protein was carried out by comparison between the molecular weights determined by LC/MS/MS and theoretical masses.

Semiquantitative RT-PCR—Total RNAs were isolated from cells with the TRIzol reagent (Invitrogen), and cDNAs were synthesized from 1 μg of each RNA preparation using the PrimeScript RT reagent kit (TakaraBio, Shiga) as described (16). To avoid saturation of PCR products, conditions of PCR were optimized before semiquantitative RT-PCR was carried out. The primers used for PCR are as follows: p21, 5′-actctcagggtcgaaaacgg-3′ (sense) and 5′-cttcctgtgggcggattagg-3′ (antisense); glyceraldehyde 3-phosphate dehydrogenase (GAPDH), 5′-accacagtccatgccatcac-3′ (sense) and 5′-tccac-

Downloaded from http://www.jbc.org/ at IYAKU KIBAN KENKYUJO on April 24, 2014

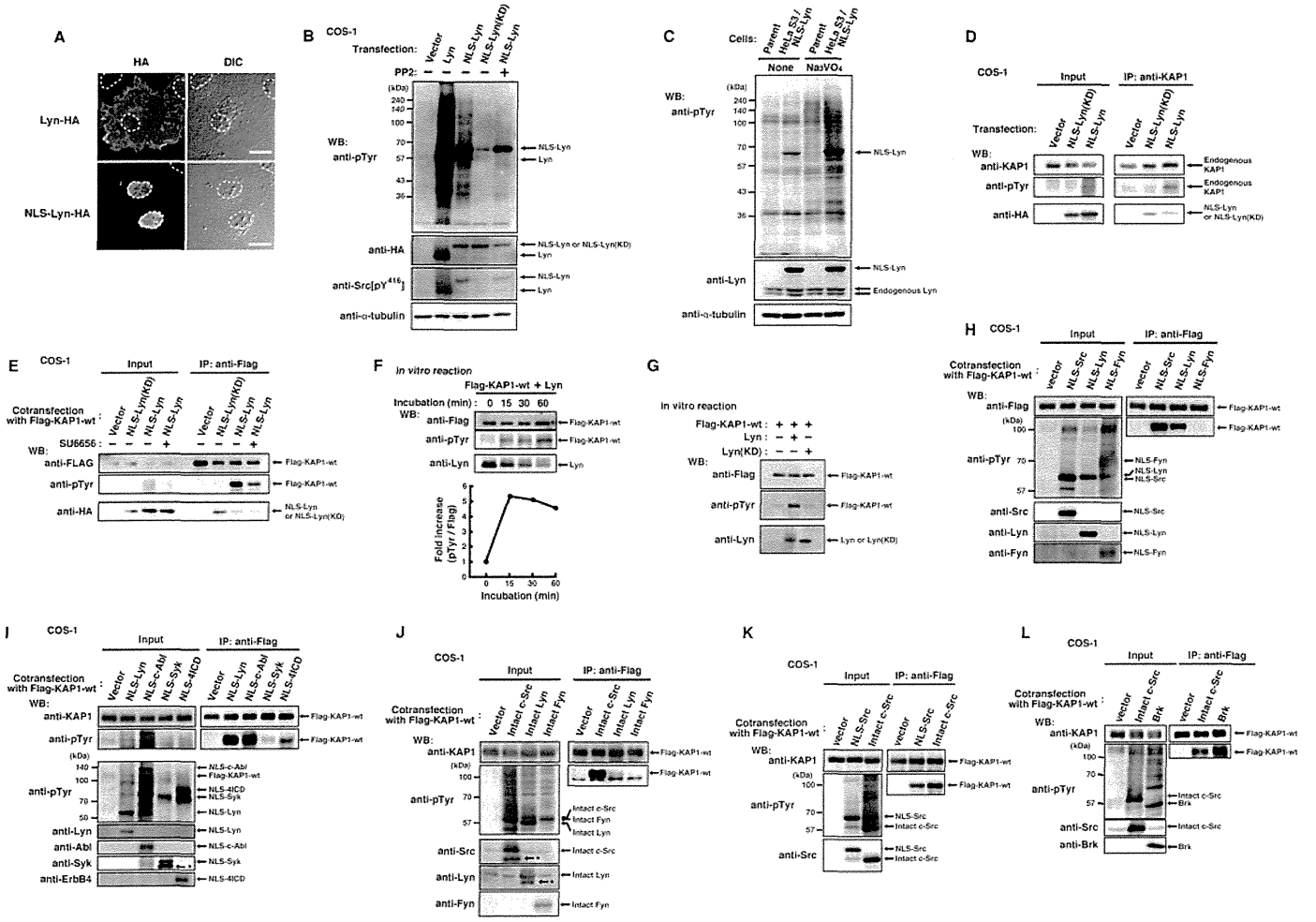


FIGURE 1. **Tyrosine phosphorylation of KAP1 induced by nuclear tyrosine kinases.** *A*, COS-1 cells transfected with Lyn-HA or NLS-Lyn-HA were cultured for 24 h. Cells were fixed and stained with anti-HA antibody. The areas of nuclei are marked by *dotted lines*. *DIC*, differential interference-contrast. *B*, COS-1 cells transfected with the indicated plasmids were cultured for 24 h in the presence or absence of 10 μM PP2 during the last 12 h. Immunoblotting (Western blot; *WB*) was performed with the indicated antibodies. *C*, parental HeLa S3 or HeLa S3/NLS-Lyn cells treated with or without 0.5 mM sodium orthovanadate (Na_3VO_4) were cultured for 1.5 h. Immunoblotting was performed with the indicated antibodies. *D*, COS-1 cells transfected with the indicated plasmids were cultured for 24 h. Endogenous KAP1 was immunoprecipitated (*IP*) with anti-KAP1 antibody. Immunoblotting was performed with the indicated antibodies. *E*, COS-1 cells cotransfected with KAP1-wt plus the indicated plasmids were cultured for 24 h in the presence of 10 μM SU6656 or DMSO (dimethyl sulfoxide, solvent control) during the last 3 h. KAP1-wt was immunoprecipitated with anti-FLAG antibody. Immunoblotting was performed with the indicated antibodies. *F*, KAP1-wt immunoprecipitates were incubated with Lyn immunoprecipitates in reaction buffer. Samples were taken at the indicated times. Immunoblotting was performed for FLAG, Tyr(P), and Lyn. The levels of tyrosine phosphorylation at each incubation time (15, 30, and 60 min) relative to that of the control (0 min) are shown. *G*, KAP1-wt immunoprecipitates were incubated with Lyn or Lyn(KD) immunoprecipitates for 30 min in reaction buffer. Immunoblotting was performed with the indicated antibodies. *H–L*, COS-1 cells cotransfected with KAP1-wt plus the indicated plasmids were cultured for 24 h. KAP1-wt was immunoprecipitated with anti-FLAG antibody. Immunoblotting was performed with the indicated antibodies. *Asterisks* show degradation products.

caccctgttgctgta-3′ (antisense) (16, 17). The sizes of PCR products are 104 bp for p21 and 452 bp for GAPDH. Amplification was carried out using an MJ mini thermal cycler (Bio-Rad) with Ex TaqDNA polymerase (TakaraBio) under the following conditions: for p21, initial heating at 94 °C for 2 min, followed by 27 cycles of denaturation at 94 °C for 30 s, annealing at 63 °C for 30 s, and extension at 72 °C for 1 min; for GAPDH, initial heating at 94 °C for 2 min, followed by 25 cycles of denaturation at 94 °C for 30 s, annealing at 56 °C for 30 s, and extension at 72 °C for 1 min. The products of RT-PCR were electrophoresed on a 2.5% agarose gel containing ethidium bromide. The density of each amplified fragment was quantitated using a ChemiDoc XRSPlus image analyzer and Quantity One software. The relative amount of p21 represents the mean ± S.D. from three independent experiments. An *asterisk* indicates the significant difference (*, $p < 0.05$) calculated by Student's *t* test (Fig. 4*H*).

RESULTS

Tyrosine Phosphorylation of KAP1—To identify tyrosine-phosphorylated proteins in the nucleus, we established cell lines expressing Lyn tyrosine kinase tagged with a nuclear localization signal (NLS-Lyn). Affinity-purified proteins using anti-Tyr(P) antibody were excised from an SDS-polyacrylamide gel and subjected to proteolytic cleavage followed by LC/MS/MS. The peptide derived from p110 exhibited 100% identity with the amino acid sequence of human KAP1 (Fig. 1, *A–C*, and supplemental Table S2), a component of chromatin structure (43).

To verify tyrosine phosphorylation of KAP1, we transfected COS-1 cells with NLS-Lyn or NLS-Lyn(KD) and immunoprecipitated endogenous KAP1 from cell lysates. Endogenous KAP1 was tyrosine-phosphorylated by NLS-Lyn but not NLS-Lyn(KD) (Fig. 1*D*). Furthermore, cells were cotransfected with KAP1-wt plus NLS-Lyn or KAP1-wt plus NLS-Lyn(KD) and cultured in the presence or absence of the SFK inhibitor SU6656. Expressed KAP1-wt was also tyrosine-phosphorylated by NLS-Lyn but not NLS-Lyn(KD), and treatment with SU6656 inhibited tyrosine phosphorylation of KAP1-wt (Fig. 1*E*). These results suggest that tyrosine phosphorylation of KAP1 is induced by NLS-Lyn. Furthermore, we tested whether Lyn directly phosphorylated KAP1 at tyrosine residues. KAP1-wt, Lyn, and Lyn(KD) were immunoprecipitated from respective transfected cells and subjected to *in vitro* kinase assays (Fig. 1, *F* and *G*). Tyrosine phosphorylation of KAP1-wt by Lyn was observed in a kinase activity-dependent manner, suggesting that Lyn directly phosphorylates KAP1 at tyrosine residues.

To examine whether the other SFK members were able to phosphorylate KAP1 at tyrosine residues, we cotransfected cells with KAP1-wt in conjunction with NLS-Lyn, NLS-Src, or NLS-Fyn, which are all localized to the nucleus (10) (Fig. 1*A*). Unlike NLS-Fyn, NLS-Src and NLS-Lyn were able to phosphorylate KAP1 at tyrosine residues (Fig. 1*H*). Previously, we showed a strong relationship between various tyrosine kinases and chromatin structural changes (10, 16, 17). Next, we examined whether the other families of tyrosine kinases were able to phosphorylate KAP1. NLS-c-Abl, NLS-Syk, and NLS-4ICD were found to phosphorylate KAP1-wt at tyrosine residues, irrespective of various levels of tyrosine phosphorylation of KAP1-wt (Fig. 1*I*).

Next, to examine the effect of the NLS sequence *per se* on KAP1 phosphorylation, we cotransfected cells with KAP1-wt in conjunction with intact c-Src, intact Lyn, or intact Fyn. Like NLS-Src, intact c-Src strongly phosphorylated KAP1-wt at tyrosine residues (Fig. 1, *H* and *J–L*). Intact Lyn also phosphorylated KAP1-wt at tyrosine residues despite the low levels of tyrosine phosphorylation (Fig. 1*J*). The levels of tyrosine phosphorylation of KAP1 were increased when NLS-Lyn was used in place of intact Lyn (Fig. 1, compare *H* with *J*). However, neither NLS-Fyn nor intact Fyn phosphorylated KAP1-wt at tyrosine residues (Fig. 1, *H* and *J*). Brk, a non-receptor-type tyrosine kinase that localizes in the nucleus, also phosphorylated KAP1-wt at tyrosine residues (Fig. 1*L*). These results suggest that KAP1 is a substrate for various tyrosine kinases that localize in the nucleus, and their nuclear localization is critical for tyrosine phosphorylation of KAP1.

Tyrosine Phosphorylation of KAP1 at Tyr-449, Tyr-458, and Tyr-517—To determine the tyrosine phosphorylation sites of KAP1, we constructed several deletion mutants of KAP1 (Fig. 2, *A* and *C*). Cells were cotransfected with NLS-Lyn plus KAP1-wt or KAP1 deletion mutants, and we found that NLS-Lyn induced tyrosine phosphorylation of KAP1(N1)(1–469) but not KAP1(C)(469–835) and KAP1(N2)(1–380) (Fig. 2, *B* and *D*). In addition, phospho-Tyr-517 on KAP1 was detected by mass spectrometry (supplemental Table S2). Given that KAP1 has only two tyrosine residues at positions 449 and 458 (Tyr-449 and Tyr-458) in the region between 380 and 469, we constructed KAP1 mutants, which are mutated at Tyr-449, Tyr-458, and Tyr-517 to phenylalanine (KAP1-Y449F, KAP1-Y458F, KAP1-Y517F, and KAP1–3YF) (Fig. 2*E*). Cotransfection of cells with NLS-Lyn plus KAP1-wt or NLS-Lyn plus KAP1 mutants showed that Tyr-449, Tyr-458, and Tyr-517 were phosphorylated to a similar extent (Fig. 2, *F* and *G*). Importantly, we found that tyrosine phosphorylation of KAP1–3YF was barely detected (Fig. 2*H*). Similar results were obtained with *in vitro* kinase assays (Fig. 2*I*). These results suggest that Tyr-449, Tyr-458, and Tyr-517 are the major tyrosine phosphorylation sites of KAP1.

Next, we examined whether various tyrosine kinases phosphorylated the same tyrosine residues of KAP1. In fact, we found that NLS-Lyn, NLS-c-Abl, NLS-Syk, and NLS-4ICD did not induce tyrosine phosphorylation of KAP1–3YF in cells cotransfected with KAP1–3YF plus each tyrosine kinase (Fig. 2*J*; see Fig. 1*I*), indicating that Tyr-449, Tyr-458, and Tyr-517 are the common tyrosine phosphorylation sites of KAP1 for various tyrosine kinases.

Inhibitory Role of Tyrosine Phosphorylation in Recruitment of KAP1 and HP1α to Chromatin—KAP1 binds to chromatin and acts as a scaffold for the assembly of heterochromatin proteins, including heterochromatin protein 1α (HP1α), that participate in heterochromatin formation (44–46). To examine the state of chromatin-bound proteins, cells were extracted with high salt buffer before fixation and immunostained for KAP1 and HP1α. Consistent with previous studies (37, 47), immunostaining showed that both endogenous KAP1 and HP1α were strongly stained within heterochromatic condensed chromatin, compared with decondensed chromatin (Fig. 3*A*). Moreover, we established KAP1 knockdown cell lines (HeLa S3/shKAP1) and immunostained for HP1α. KAP1 knockdown was found to decrease the levels of chromatin-bound HP1α (Figs. 3*A* and 4*B*). These results substantiate the co-association of KAP1 and HP1α within heterochromatin.

To examine the effect of nuclear tyrosine phosphorylation on KAP1 binding to chromatin, we transfected HeLa S3 cells with NLS-Lyn and immunostained for chromatin-bound KAP1. Intriguingly, the levels of chromatin-bound KAP1 were decreased upon NLS-Lyn expression (Fig. 3*B*). Furthermore, we immunostained for chromatin-bound HP1α and found that upon NLS-Lyn expression, the levels of chromatin-bound HP1α were decreased within heterochromatic condensed chromatin as well as those of chromatin-bound KAP1 (Fig. 3, *B* and *C*). These results suggest that nuclear tyrosine phosphorylation inhibits recruitment of KAP1 and HP1α to heterochromatin.

Effect of Tyrosine Phosphorylation on the Association of KAP1 with Heterochromatin—To examine whether nuclear tyrosine phosphorylation inhibited KAP1 association with heterochromatin, cells were subfractionated into the low salt soluble fraction, the high salt soluble fraction, and the insoluble fraction (see "Experimental Procedures"). The low salt soluble fraction contained the cytosolic protein $cPLA_2$, and the high salt soluble fraction contained the chromatin-binding protein Ku70 (Fig. 3*D*). The insoluble fraction, which we focused on, contained the nuclear matrix protein lamin A/C and the heterochromatin protein HP1α. KAP1 was distributed into the low salt soluble

Downloaded from http://www.jbc.org/ at IYAKU KIBAN KENKYUJO on April 24, 2014

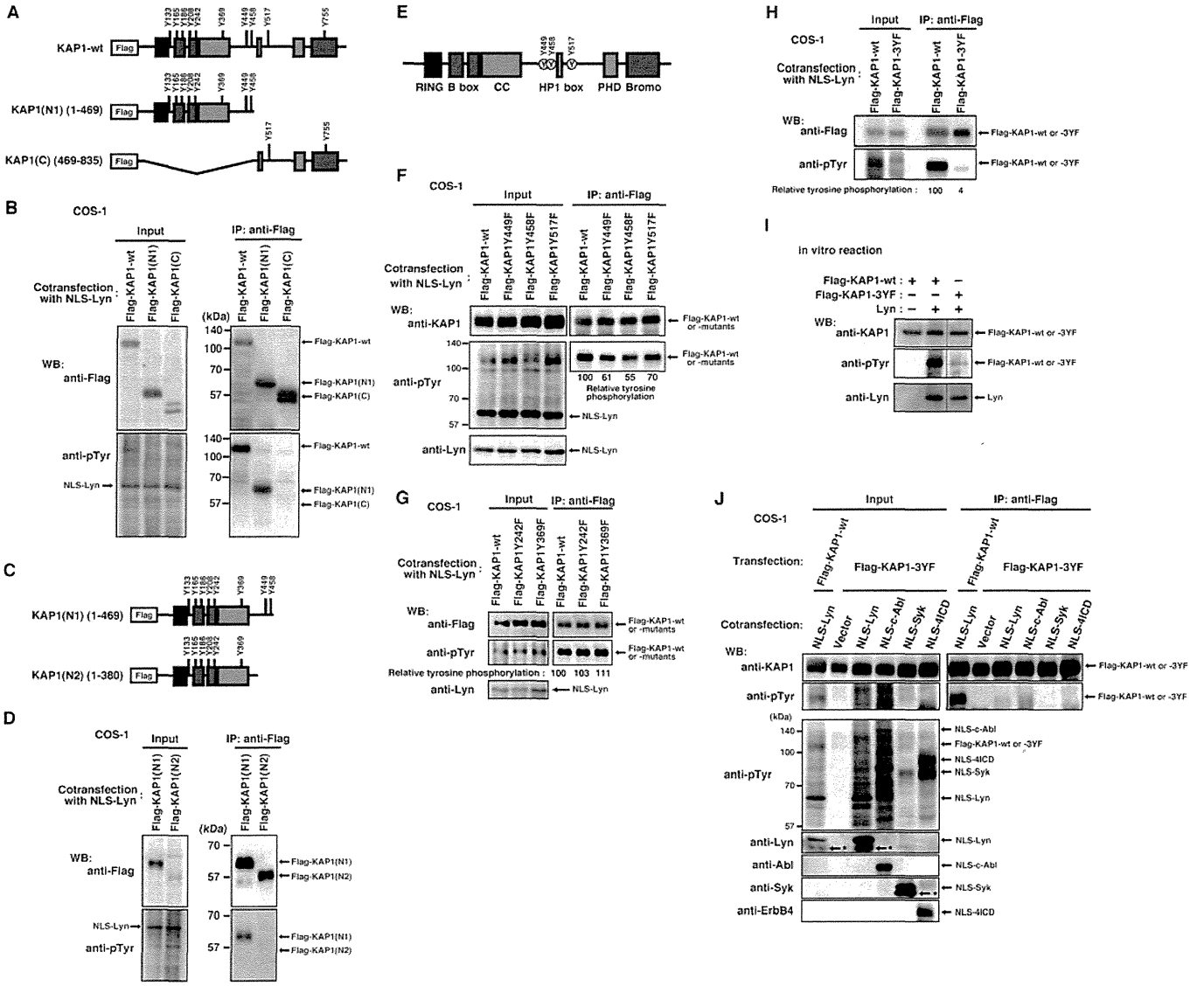


FIGURE 2. **Tyrosine phosphorylation of KAP1 at Tyr-449, Tyr-458, and Tyr-517.** *A*, *C*, *E*, a schematic representation of KAP1. *RING*, RING finger domain; *B box*, B box zinc fingers 1 and 2; *CC*, coiled-coil domain; *HP1 box*, heterochromatin protein 1 box; *PHD*, plant homeodomain; *Bromo*, Bromo domain. *B*, *D*, and *F–H*, COS-1 cells cotransfected with NLS-Lyn plus the indicated plasmids were cultured for 24 h. KAP1-wt and its mutants were immunoprecipitated (*IP*) with anti-FLAG antibody. Immunoblotting (*WB*) was performed with the indicated antibodies. *I*, KAP1-wt or KAP1–3YF immunoprecipitates were incubated with Lyn immunoprecipitates, as described in the legend to Fig. 1*G*. Immunoblotting was performed with the indicated antibodies. *J*, COS-1 cells cotransfected with KAP1-wt plus NLS-Lyn or KAP1–3YF plus the indicated plasmids were cultured for 24 h. KAP1-wt and KAP1–3YF were immunoprecipitated with anti-FLAG antibody. Immunoblotting was performed with the indicated antibodies. *Asterisks* show degradation products.

fraction, the high salt soluble fraction, and the insoluble fraction (Fig. 3*D*), confirming that KAP1 is a component of heterochromatin, but not all of KAP1 associates with heterochromatin. In fact, nearly 25% of KAP1 binds to highly compacted heterochromatin (48). We subfractionated parental and NLS-Lyn-expressing cells and found that the amounts of endogenous KAP1 were decreased in the insoluble fraction upon NLS-Lyn expression, although the protein levels of KAP1 in whole cells were almost unchanged irrespective of NLS-Lyn expression (Fig. 3*E*; see also Fig. 3*K*). These results suggest that the association of KAP1 with heterochromatin is inhibited upon NLS-Lyn expression.

Next, we examined the inhibitory role of NLS-Lyn kinase activity in the association of KAP1 with heterochromatin. Treatment with SU6656 inhibited the NLS-Lyn-mediated decrease in the amounts of endogenous KAP1 in the insoluble fraction (Fig. 3*F*). Upon NLS-Lyn(KD) expression, the amounts of endogenous KAP1 were not decreased in the insoluble fraction (Fig. 3*G*). These results suggest that the tyrosine kinase activity is critical for a decrease in the levels of KAP1 association with heterochromatin.

Next we examined whether c-Src, which strongly phosphorylated KAP1 (see Fig. 1*J*), decreased the amounts of KAP1 in the insoluble fraction. We subfractionated HeLa S3 cells inducibly expressing v-Src, a highly activated variant of c-Src. The amounts of endogenous KAP1 were decreased in the insoluble fraction when v-Src was induced, and the decrease was inhibited by SU6656 treatment (Fig. 3*H*). Furthermore, we found that the amounts of HP1α were decreased in the insoluble fraction in a kinase activity-dependent manner as well as those of

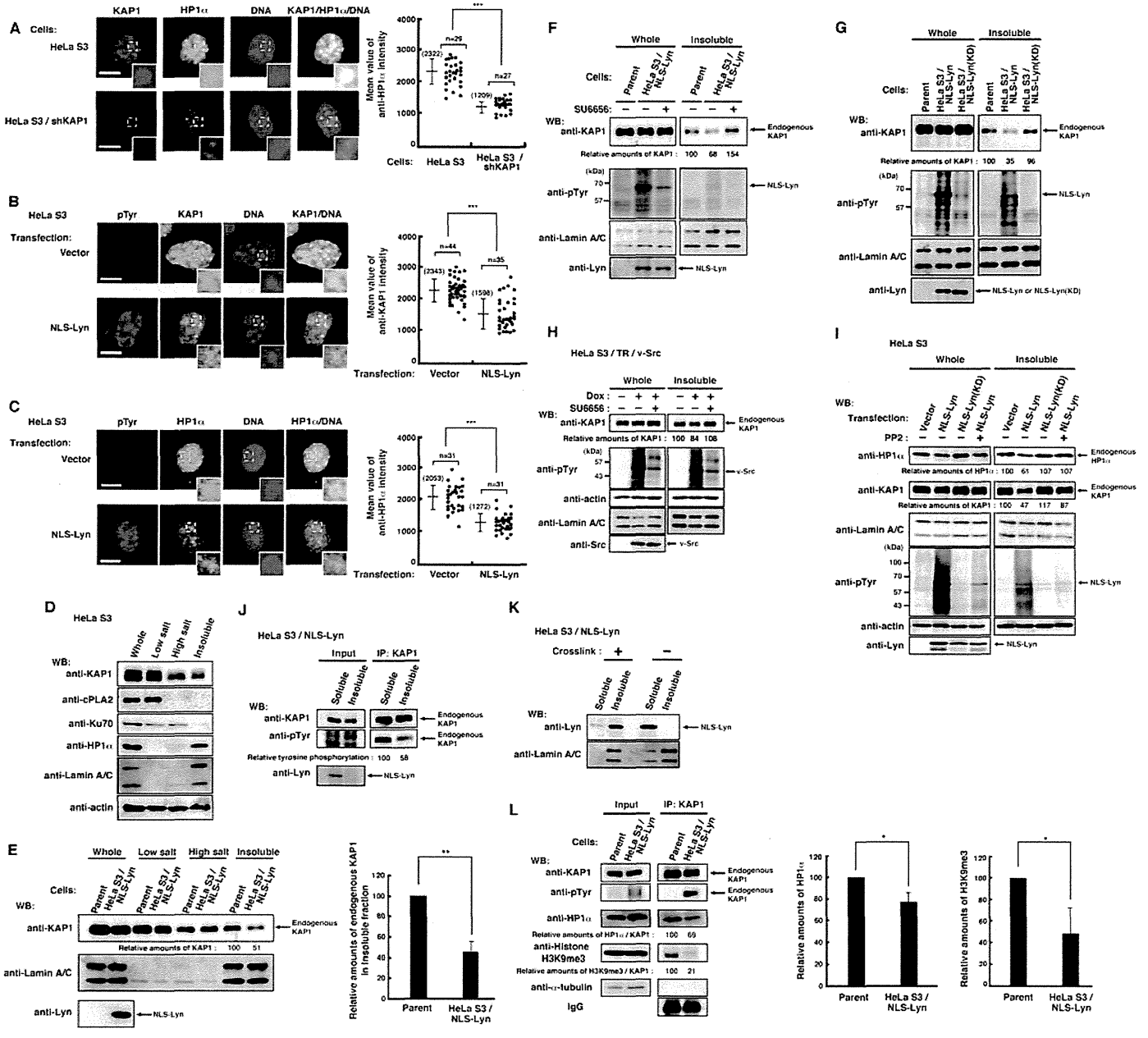


FIGURE 3. **Decrease in the levels of KAP1 association with heterochromatin induced by nuclear tyrosine phosphorylation.** *A*, parental HeLa S3 cells or HeLa S3/shKAP1 cells were extracted, fixed, and triply stained with the indicated antibodies and PI. The plot represents the mean intensity of anti-HP1α staining in each cell. *B* and *C*, HeLa S3 cells transfected with vector or NLS-Lyn were cultured for 24 h. Cells were extracted, fixed, and triply stained with the indicated antibodies and PI. The plot represents the mean fluorescence intensity of anti-KAP1 (*B*) or anti-HP1α (*C*) staining in each cell. *D*, HeLa S3 cells were subjected to subcellular fractionation. Immunoblotting (*WB*) was performed with the indicated antibodies. *E*, parental HeLa S3 or HeLa S3/NLS-Lyn cells treated with 0.5 mM Na_3VO_4 were cultured for 1.5 h. Cells were subjected to subcellular fractionation. Immunoblotting was performed with the indicated antibodies. Relative amounts of KAP1 were quantitated. *Error bars*, S.D. *F–I*, cells were subjected to subcellular fractionation. Immunoblotting was performed with the indicated antibodies. *F*, parental HeLa S3 or HeLa S3/NLS-Lyn cells treated with SU6656 or DMSO for 3 h were cultured in the presence of 0.5 mM Na_3VO_4 during the last 1.5 h. *G*, parental HeLa S3, HeLa S3/NLS-Lyn, or HeLa S3/NLS-Lyn(KD) cells treated with 0.5 mM Na_3VO_4 were cultured for 1.5 h. *H*, HeLa S3/TR/v-Src cells treated with or without doxycycline (*Dox*) were cultured for 24 h in the presence of DMSO or SU6656 during the last 12 h. *I*, HeLa S3 cells transfected with the indicated plasmids were cultured for 36 h in the presence or absence of 10 μM PP2 during the last 24 h. *J*, HeLa S3/NLS-Lyn cells treated with 0.5 mM Na_3VO_4 were cultured for 1.5 h. Cells were subjected to subcellular fractionation. The insoluble fraction was suspended in high salt buffer and solubilized by sonication. Endogenous KAP1 was immunoprecipitated (*IP*) with anti-KAP1 antibody from the soluble and the insoluble fractions. Immunoblotting was performed with the indicated antibodies. *K*, HeLa S3/NLS-Lyn cells were cross-linked in medium containing 1% paraformaldehyde and incubated at 4 °C for 15 min. The cross-linking reaction was stopped by adding glycine to 0.125 M. Cells were subjected to subcellular fractionation. Immunoblotting was performed with the indicated antibodies. *L*, parental HeLa S3 or HeLa S3/NLS-Lyn cells treated with 0.5 mM Na_3VO_4 were cultured for 1.5 h and extracted by low salt buffer. The resultant insoluble fraction was suspended in high salt buffer, solubilized by sonication. Endogenous KAP1 was immunoprecipitated with anti-KAP1 antibody. Immunoblotting was performed with the indicated antibodies. Relative amounts of HP1α and histone H3K9me3 were quantitated.

KAP1 (Fig. 3*I*). These results suggest that nuclear tyrosine phosphorylation decreases the association of KAP1 and HP1α with heterochromatin.

To examine whether tyrosine-phosphorylated KAP1 decreased its association with heterochromatin, we compared the tyrosine phosphorylation levels of KAP1 in the soluble fraction

Downloaded from http://www.jbc.org/ at IYAKU KIBAN KENKYUJO on April 24, 2014

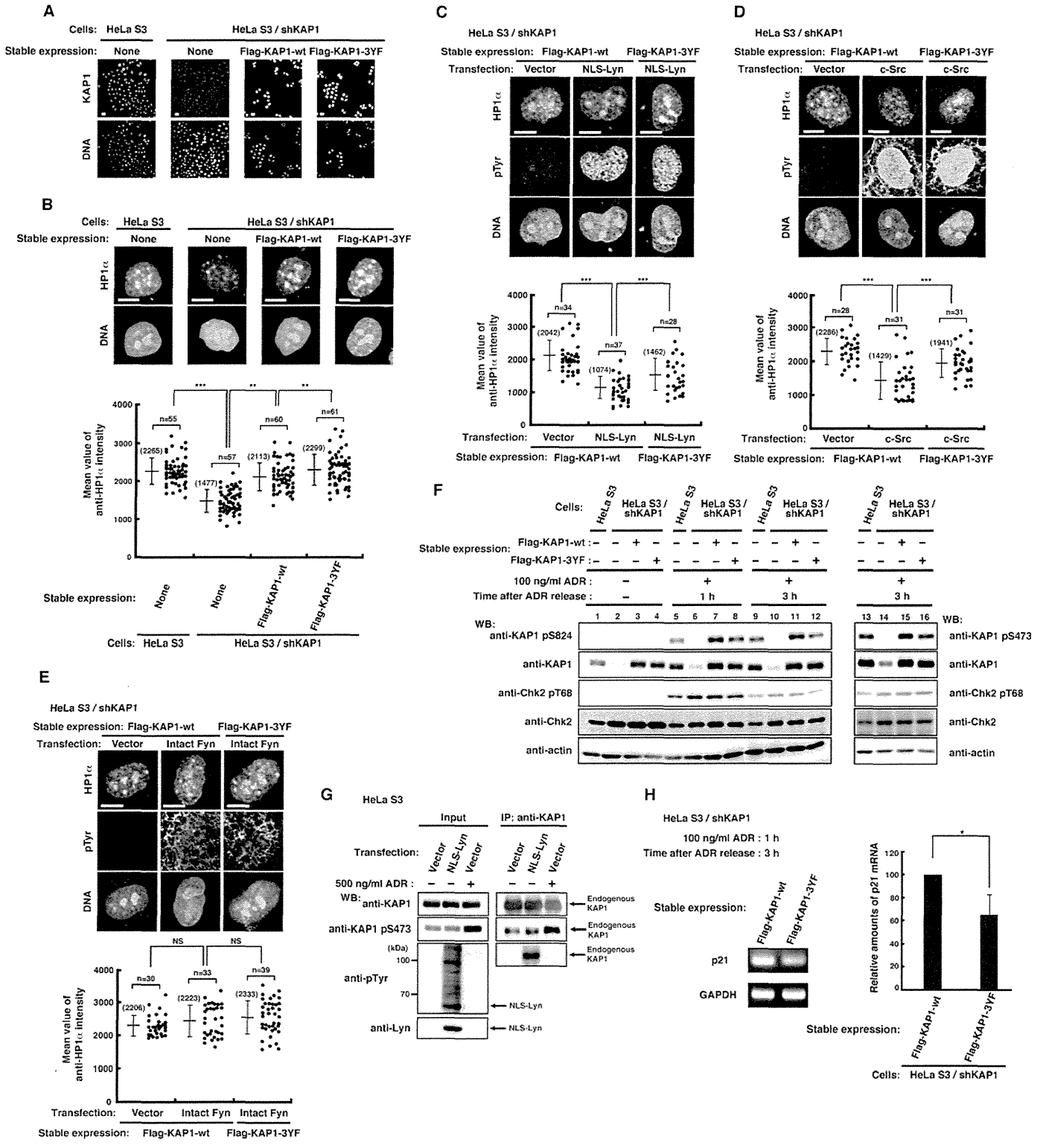


FIGURE 4. **Effect of tyrosine phosphorylation of KAP1 at Tyr-449, Tyr-458, and Tyr-517 on the association of HP1α with chromatin.** *A*, parental HeLa S3 cells or HeLa S3/shKAP1 cells in which endogenous KAP1 had been knocked down and replaced with KAP1-wt or KAP1–3YF were fixed and doubly stained with anti-KAP1 antibody and PI. *B*, cells were extracted, fixed, and doubly stained with anti-HP1α antibody and PI. The plot represents the mean intensity of anti-HP1α staining in each cell. *C–E*, HeLa S3/shKAP1 cells expressing KAP1-wt or KAP1–3YF were transfected with the indicated plasmids and cultured for 36 h. Cells were extracted, fixed, and triply stained with the indicated antibodies and TOPRO-3. The plot represents the mean intensity of anti-HP1α staining in each cell. *F*, HeLa S3/shKAP1 cells expressing KAP1-wt or KAP1–3YF were treated with 100 ng/ml ADR for 1 h and lysed at the indicated times after the removal of ADR. Immunoblotting (*WB*) was performed with the indicated antibodies. *G*, HeLa S3 cells transfected with vector or NLS-Lyn were cultured for 24 h. Cells treated with DMSO or 500 ng/ml ADR for 1 h were cultured for 3 h after the removal of ADR or DMSO. Endogenous KAP1 was immunoprecipitated (*IP*) with anti-KAP1 antibody. Immunoblotting was performed with the indicated antibodies. *H*, cells were treated as described in *F*. The levels of p21 expression were assessed by semiquantitative RT-PCR, and the amounts of p21 product were quantitated by measuring band intensities and normalizing to the levels of GAPDH. *Error bar*, S.D.

with those in the insoluble fraction. The tyrosine phosphorylation levels of endogenous KAP1 in immunoprecipitates from the soluble fraction were about 2 times as high as those from the insoluble fraction (Fig. 3, *J* and *K*). Then we examined the effect of NLS-Lyn on KAP1 association with HP1α and H3K9me3 (44, 45, 49). HP1α and H3K9me3 were coimmunoprecipitated with endogenous KAP1, and we found that the amounts of HP1α and H3K9me3 coimmunoprecipitated with KAP1 were decreased when KAP1 was tyrosine-phosphorylated (Fig. 3*L*). These results suggest that tyrosine phosphorylation of KAP1 impairs its association with heterochromatin.

Inhibitory Role of Tyrosine Phosphorylation of KAP1 at Tyr-449, Tyr-458, and Tyr-517 in HP1α Association with Chromatin—Tyrosine phosphorylation of KAP1 decreased the amounts of chromatin-bound KAP1 and HP1α (Fig. 3, *B* and *C*). To examine the effect of tyrosine phosphorylation of KAP1 at Tyr-449, Tyr-458, and Tyr-517 on HP1α association with chromatin, endogenous KAP1 was complemented by stable expression of shRNA-resistant KAP1-wt or KAP1–3YF in HeLa S3/shKAP1 cells. We confirmed the expression of shRNA-resistant KAP1 in these cell lines with immunostaining and Western blotting (Fig. 4, *A* and *F*). HeLa S3 cells, HeLa S3/shKAP1 cells, and HeLa S3/shKAP1 cells expressing KAP1-wt or KAP1–3YF were immunostained for HP1α. KAP1 knockdown decreased the amounts of chromatin-bound HP1α (Fig. 4*B*; see also Fig. 3*A*). It is of note that the levels of chromatin-bound HP1α in KAP1–3YF-expressing cells were significantly increased compared with those in KAP1-wt-expressing cells (Fig. 4*B*). To further ascertain the effect of tyrosine phosphorylation of KAP1 at Tyr-449, Tyr-458, and Tyr-517 on HP1α association with chromatin, HeLa S3/shKAP1 cells expressing KAP1-wt or KAP1–3YF were transfected with NLS-Lyn. The amounts of chromatin-bound HP1α were decreased in KAP1-wt-expressing cells upon NLS-Lyn expression, and the decrease was inhibited in KAP1–3YF-expressing cells (Fig. 4*C*). These results suggest that phosphorylation of KAP1 at Tyr-449, Tyr-458, and Tyr-517 has an inhibitory role in HP1α association with chromatin.

Next, HeLa S3/shKAP1 cells expressing KAP1-wt or KAP1–3YF were transfected with c-Src or Fyn. c-Src, which strongly phosphorylated KAP1, induced a decrease in the amounts of chromatin-bound HP1α in KAP1-wt-expressing cells, and the decrease was inhibited in KAP1–3YF-expressing cells (Fig. 4*D*; see also Fig. 1*J*). In contrast to c-Src, Fyn, which did not phosphorylate KAP1, had no effect on HP1α association with chromatin (Fig. 4*E*; see also Fig. 1*J*). Intriguingly, tyrosine phosphorylation mediated by c-Src was detected in the nucleus, but tyrosine phosphorylation mediated by Fyn was detected largely in the cytoplasm (Fig. 4, *D* and *E*). These results suggest that c-Src decreases HP1α association with chromatin through phosphorylation of KAP1 at Tyr-449, Tyr-458, and Tyr-517 in the nucleus.

KAP1 phosphorylation at serine 824 (Ser(P)-824) by ATM and at serine 473 (Ser(P)-473) by Chk2 plays important roles in DNA damage responses (27, 37, 50), and the tyrosine kinases Lyn and c-Abl are activated in DNA damage responses (51, 52). We thus examined the effect of KAP1 tyrosine phosphorylation on KAP1-Ser(P)-824 and KAP1-Ser(P)-473. HeLa S3 cells, HeLa S3/shKAP1 cells, and HeLa S3/shKAP1 cells expressing KAP1-wt or KAP1–3YF were treated with the DNA-damaging agent ADR. The levels of Ser(P)-824 and Ser(P)-473 of KAP1–3YF were found to be lower than those of KAP1-wt (Fig. 4*F*, compare *lane 7* with *lane 8*, *lane 11* with *lane 12*, and *lane 15* with *lane 16*). However, the levels of KAP1-Ser(P)-473 were not changed without DNA damage, irrespective of tyrosine phosphorylation of KAP1 (Fig. 4*G*). These results suggest that tyrosine phosphorylation of KAP1 at Tyr-449, Tyr-458, and Tyr-517 is involved in phosphorylation of KAP1 at Ser-824 and Ser-473 in DNA damage responses.

Because phosphorylation of KAP1 at Ser-824 and Ser-473 is required for transcription of p21 in DNA damage responses (50), we analyzed the expression levels of the p21 mRNA in HeLa S3/shKAP1 cells expressing KAP1-wt or KAP1–3YF treated with ADR. Semiquantitative RT-PCR analysis showed that the levels of p21 gene expression were decreased in KAP1–3YF expressing cells compared with KAP1-wt expressing cells (Fig. 4*H*). These results suggest that tyrosine phosphorylation of KAP1 at Tyr-449, Tyr-458, and Tyr-517 is involved in DNA damage responses.

DISCUSSION

In the present study, we show that KAP1 is phosphorylated at Tyr-449, Tyr-458, and Tyr-517. These three tyrosine residues are the common tyrosine phosphorylation sites of KAP1 for various tyrosine kinases that are localized within the nucleus. We further show that tyrosine phosphorylation of KAP1 decreases its association with heterochromatin, which is accompanied by a decrease in the amounts of chromatin-bound HP1α.

Previous reports showed post-translational modifications of KAP1 and its importance for proper functions. Phosphorylation of KAP1 at Ser-473 decreases its association with HP1, and phosphorylation at Ser-824 relaxes chromatin structure (27, 53). SUMOylation of KAP1 is required for gene silencing (54). Although tyrosine phosphorylation of KAP1 is reported to be induced by c-Fes tyrosine kinase (55) and PDGF stimulation (56), the major tyrosine phosphorylation sites of KAP1 have not been identified thus far, and the roles of tyrosine phosphorylation of KAP1 are largely unknown.

We have been studying nuclear tyrosine phosphorylation and the effect of nuclear tyrosine phosphorylation on chromatin structural changes. Chk tyrosine kinase localizes within the nucleus and brings about growth retardation and aberrant chromosome movement leading to multinucleation (14, 57). SFK and c-Abl tyrosine kinase localized in the nucleus induce chromatin structural changes (10, 16). In this study, to understand the regulatory mechanism of chromatin structural changes through tyrosine phosphorylation, we tried to identify nuclear tyrosine-phosphorylated proteins by mass spectrometry. Tyrosine phosphorylation induced by NLS-Lyn was barely detected without Na_3VO_4, an inhibitor of tyrosine phosphatases (Fig. 1*C*). We thus incubated NLS-Lyn-expressing cells in medium supplemented with Na_3VO_4 (Fig. 1*C*), because tyrosine phosphatases may be abundant in the nucleus (4). Taken together with the fact that Na_3VO_4 treatment greatly increases nuclear tyrosine phosphorylation (10), these results suggest

Downloaded from http://www.jbc.org/ at IYAKU KIBAN KENKYUJO on April 24, 2014